A FAST AND ACCURATE AUTOMATED PAVEMENT CRACK DETECTION ALGORITHM

A Dissertation
Presented to
The Academic Faculty

By

Anirban Chatterjee

In Partial Fulfillment
of the Requirements for the Degree
Master of Science in Computational Science and Engineering
School of Civil and Environmental Engineering

Georgia Institute of Technology

December 2017

A FAST AND ACCURATE AUTOMATED PAVEMENT CRACK DETECTION ALGORITHM

Approved by:

Dr. Yi-Chang (James) Tsai, Advisor
School of Civil and Environmental Engineering
Georgia Institute of Technology

Dr. James Lai
School of Civil and Environmental Engineering
Georgia Institute of Technology

Dr. Ümit V. Çatalyürek
School of Computational Science and Engineering
Georgia Institute of Technology

Date Approved: October 19, 2017

To my family.

ACKNOWLEDGEMENTS

Firstly, I would like to thank my advisor, Dr. Yi-Chang Tsai, for his support. He gave me the opportunity to tie my background in transportation engineering to my passion for computer vision for which I shall forever be grateful. His guidance and confidence in me has helped to make this research possible.

I would also like to thank my committee members, Dr. James Lai and Dr. Ümit V. Çatalyürek for serving as my committee members and providing valuable feedback which has helped to shape this dissertation.

I would also like to express my appreciation to our research group, especially Dr. Zhaohua Wang, Dr. Yi-Ching Wu and Dr. Chengbo Ai for their constant support and feedback.

Finally, I am grateful to my family, for their support and confidence in me.

TABLE OF CONTENTS

Acknowledgments iv

List of Tables vii

List of Figures viii

Chapter 1: Introduction and Background 1

1.1 Literature Review 2

1.1.1 Overview of Pavement Crack Detection 2

1.1.2 Trends in Crack Detection Research 6

1.2 Objectives and Scope 7

Chapter 2: Technical Approach 9

2.1 Data Collection 9

2.2 Proposed Algorithm 10

2.2.1 Preprocessing 12

2.2.2 Preliminary Crack Segmentation 12

2.2.3 Crack Object Connection 15

2.2.4 Minimal Path Crack Detection 20

2.3 Demonstration 21

Chapter 3: Results 24

3.1 Accuracy 24

3.1.1 Crack Detection Algorithm - Performance Evaluation System (CDA-PES) 24

3.1.2 CDA-PES Results 29

3.1.3 Comparison to existing algorithms 29

3.2 Computation Speed 32

3.2.1 Computation Time Breakdown 32

3.2.2 Comparison with the state of the art 34

Chapter 4: Conclusion 35

4.1 Contributions 35

4.2 Future Recommendations 35

References 47

LIST OF TABLES

1.1 Crack detection algorithm literature by approach 7

2.1 Parameter values 20

3.1 Comparison of overall CDA-PES scores [111] 32

LIST OF FIGURES

1.1 Distribution of pavement distresses by deduct value 2

1.2 Distribution of pavement distresses by extent 3

1.3 Disjoint crack segmentation from individual classification 5

1.4 Number of papers on crack detection or classification published in a year . . 6

1.5 Papers published using different approaches to crack detection 8

2.1 Georgia Tech Survey Vehicle (GTSV) 10

2.2 Pavement images captured by 3D laser scanner on GTSV 11

2.3 Proposed crack detection algorithm steps 11

2.4 Effect of preprocessing 12

2.5 Result of preliminary crack segmentation 15

2.6 Crack objects overlay on preliminary image segmentation 17

2.7 Elongated crack objects overlay on preliminary image segmentation 18

2.8 Removal of false positives 19

2.9 Demonstration of proposed algorithm on image with longitudinal crack . . 22

2.10 Demonstration of proposed algorithm on image with longitudinal crack . . 23

3.1 Categories in the CDA-PES pavement image dataset 26

3.2 Different pavement types: (a) Dense graded asphalt pavement range image; (b) Crack map detected by relaxation thresholding on Figure 3.2a; (c) open graded friction course asphalt pavement range image; (d) Crack map detected by relaxation thresholding on Figure 3.2c; (e) Concrete pavement; (f) Crack map detected by relaxation thresholding on Figure 3.2e 27

3.3 Different crack types: (a) no cracking; (b) longitudinal crack; (c) transverse crack; (d) combination of crack types; (d) alligator cracking 27

3.4 Different crack widths: (a) 1 pixel crack width; (b) Canny edge detection result on Fig 3.4a; (c) 2 pixel crack width; (d) Canny edge detection result on fig 3.4c; (e) 5 pixel crack width; (f) Canny edge detection on Fig 3.4e; (g) 10 pixel crack width; (h) Canny edge detection on Fig 3.4g 28

3.5 Different crack complexities: (a) low pattern complexity; (b) medium pattern complexity; (c) high pattern complexity 28

3.6 Dashboard for proposed algorithm 30

3.7 Dashboard for tensor voting based MPS algorithm [34] 31

3.8 Computation time of proposed algorithm 33

3.9 Distribution of computation time of proposed algorithm 33

3.10 Comparison of computation time 34

SUMMARY

The US Federal Highway Trust Fund spent USD 42.95 Billion in 2015 out of which the principal expenditure was the maintenance of existing highway infrastructure. To optimize the use of resources for infrastructure maintenance, regular road infrastructure condition surveys are required. Automated road condition surveys involve the use of survey vehicles to collect road infrastructure condition data and distress detection algorithms to automatically assess the infrastructure condition. These automated road condition surveys provide a safe and efficient alternative to manual road condition surveys. However, widespread adoption of automated road condition surveys is yet to be realized.

One problem is the lack of robust, accurate and fast algorithms to detect pavement distresses. Pavement cracking is by far the most widespread and serious distress on road infrastructure. Although some crack detection algorithms have been developed to provide a high level of accuracy, their computation time makes them infeasible to implement in real-time, leading to the costly requirement of saving a large volume of road infrastructure condition data for processing at a later stage. Thus, a crack detection algorithm is required which retains accuracy in a wide range of pavement conditions without being computationally intensive.

To meet this research need, this thesis presents a fast and accurate crack detection algorithm. A minimal path based approach has been used to develop the crack detection algorithm. The technical approach consists of the following major steps: 1) Image preprocessing to remove isolated noise; 2) Preliminary crack segmentation to minimize false negatives; 3) Crack object generation and connection to remove false positives; and 4) Refinement of the crack segmentation through a minimal path search based procedure.

The Crack Detection Algorithm Performance Evaluation System (CDA-PES) has been used to validate the performance of the proposed algorithm. This thesis also compares the proposed algorithm with the previous state-of-the-art algorithm. The proposed algo-

rithm outperforms all previous algorithms tested using the CDA-PES. Additionally, the proposed algorithm achieves on average a 36 times faster computation speed than the existing state-of-the-art algorithm and a 58 times faster median computation speed. With a median processing time of 0.52 seconds for 0.65 megapixel images on a single CPU thread, this algorithm makes accurate, real-time processing viable.

The research presented in this thesis contributes significantly towards more widespread adoption of safer and efficient automated road condition surveys.

CHAPTER 1
INTRODUCTION AND BACKGROUND

The US Federal Highway Trust Fund spent USD 42.95 Billion [1] in 2015 out of which the principal expenditure was the maintenance of existing highway infrastructure. To optimize the use of resources for infrastructure maintenance, regular road infrastructure condition surveys are required. These road infrastructure condition surveys can be manual, semi-automated or automated.

In manual surveys, engineers determine the infrastructure condition during the survey on the field. This approach is unsafe, laborious and time-consuming. In semi-automated surveys, the road infrastructure is recorded using on-vehicle sensors and analyzed manually at the office. This makes the surveys safer but still laborious and time-consuming. Automated surveys involve the use of on-vehicle sensors and distress detection algorithms to automatically determine the pavement condition. Automated surveys [2] are clearly the preferred alternative. However, very few transportation agencies have adopted automated road infrastructure condition surveys.

The Georgia DOT defines deduct values as quantifications of the adverse impact on road infrastructure by various pavement distresses. The various deduct values are subtracted from a value of 100 to obtain a condition rating for a 1-mile roadway segment. Maintenance, repair and rehabilitation tasks are then prioritized based on the condition ratings of roadway segments. As shown in figure 1.1, pavement cracking (load cracking, block cracking, reflection cracking and edge cracking) has the highest impact on pavement condition, more than all other distresses combined. Figure 1.2 demonstrates the extent of various distresses. Note that a particular location can suffer from multiple distresses at once. Again, cracking is one of the most widespread pavement distresses. 76% of segments (1-mile pieces of roadway defined by Georgia Department Of Transportation for mainte-

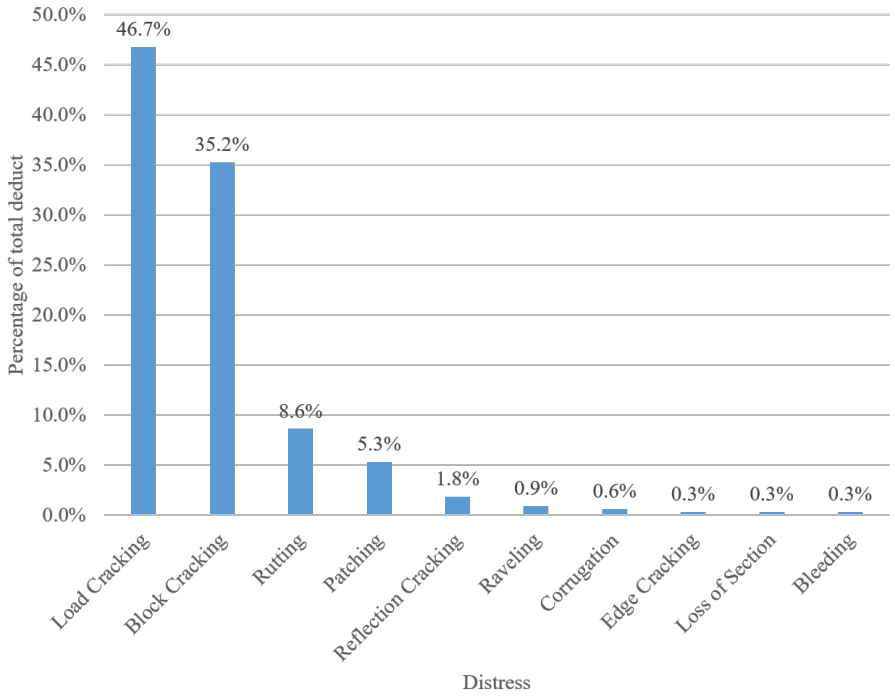

Figure 1.1: Distribution of pavement distresses by deduct value

nance purposes) suffered from some form of cracking in 2016. The following literature review summarizes research on pavement crack detection.

1.1 Literature Review

In this literature review, 104 papers pertaining to crack detection methods, or pavement distress detection methods which can be employed for crack detection, were studied. This review first discusses the crack detection problem and classifies the solutions. This is followed by an analysis of the trends in crack detection research.

1.1.1 Overview of Pavement Crack Detection

Crack detection algorithms can provide output features at different levels of detail. Some algorithms simply classify an image as cracked or uncracked. This output can help to obtain a basic idea of the proportion of roadways suffering from cracking of any kind. It can also help to reduce the manual crack detection effort. However, this output is not useful to users

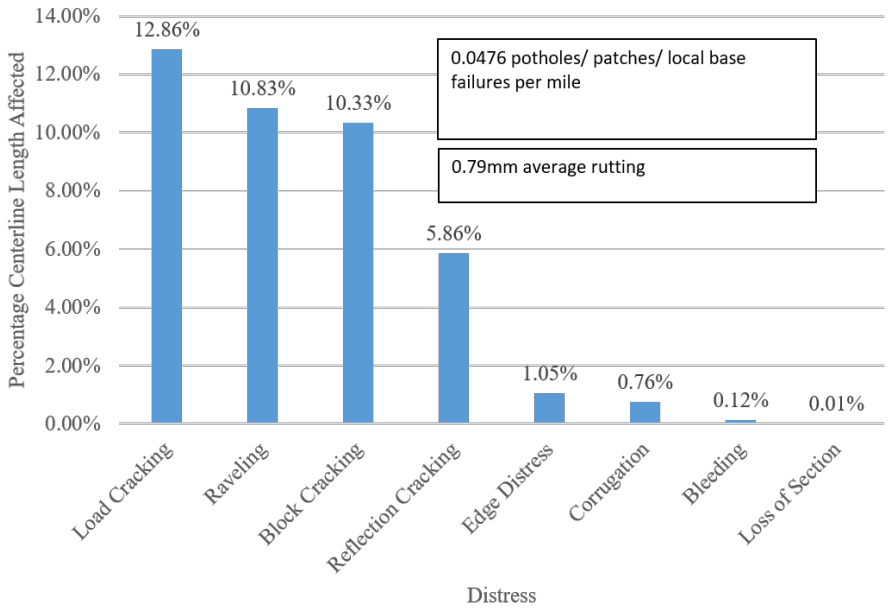

Figure 1.2: Distribution of pavement distresses by extent

requiring a more detailed description of the crack properties. Properties such as crack type, crack length, cracked area and crack width are required to quantify the pavement condition [3] and for subsequent MR&R decision-making. Algorithms which provide a greater level of detail segment image blocks or individual pixels as cracked or uncracked. This review focuses on crack detection algorithms which can provide a level of detail such that the desired crack properties can be practically determined from the output features.

The most common approach to crack detection is based on classifying image blocks or individual pixels as cracked or non-cracked, based on the aggregate statistics of the entire image or the neighborhood of the image blocks or pixels under question. Each image block or pixel is treated as a separate classification problem. Hence, the continuity of crack features is not guaranteed. This approach will be referred to as individual classification. Koutsopoulos et al. [4] compared four fast and simple individual classification algorithms: Otsu's method, Kittler's method, a relaxation method and a regression-based method. The regression-based method gave the best performance out of these methods by learning to determine an intensity threshold based on the mean and variance of the image. All of these

approaches use a single threshold for the entire image, which is often not feasible given the gradual changes in intensity because of the cross-slope of the pavement, especially in asphalt concrete pavements. Using thresholds which changed according to the neighborhood of each pixel or image block [5, 6] provided a solution to this problem. Conditional texture anisotropy (CTA) [7] also works well for identifying individual crack pixels by detecting pixels with a neighborhood which extend along a certain orientation. Free-form anisotropy [8] modifies CTA to improve its performance on irregular pavement crack patterns.

Supervised learning has also been extensively for crack detection using individual classification. Cheng et al. [9, 10] utilize an artificial neural network to determine the optimal intensity threshold for crack segmentation. Convolutional neural networks designed for pixel-wise image segmentation [11] have been used for crack detection as well [12].

Individual classification can also be applied to the frequency domain transform of the image. Thin cracks and the edges of wide cracks have sharp gradients. Edge detection methods such as Canny edge detection [13] has been applied extensively for pavement crack detection [14, 15, 16]. Mallat and Zhong (1992) [17] proposed a decimated fast bi-orthogonal wavelet transform to obtain an image edge representation by computing the local maximum of the gradient of an image. This concept has been applied extensively for crack detection at multiple scales [18, 19, 20, 21, 22, 23, 24].

As mentioned before, individual classification does not consider that cracks are continuous, salient features. As a result, the crack segmentation generally provides a disjoint crack pattern, as shown in figure 1.3. Small indentations on the pavement surface are also often misclassified as cracks, despite not being long, continuous features. Post-processing can be used to connect these disjoint crack features and to eliminate noise. These approaches will be referred to as bottom-up approaches in this review. The simplest bottom-up approach is a closing operation [25] which has been applied to crack detection [26, 27]. The closing operation however, connects noise close to the cracks as well. Hence, it is important to guide the direction of expansion along the crack structure. Some crack detection algo-

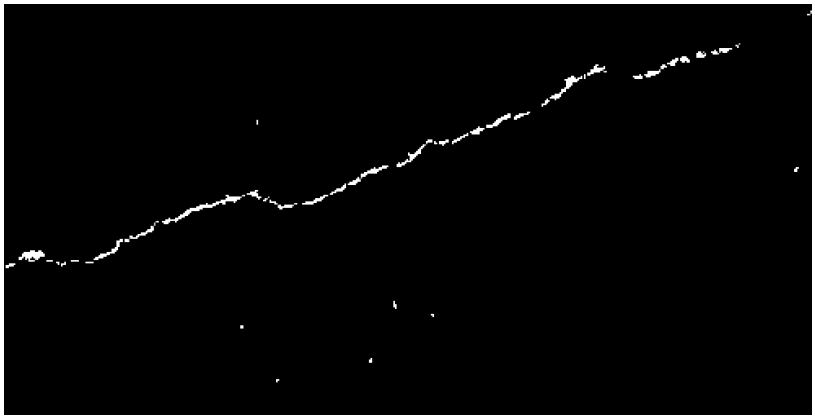

Figure 1.3: Disjoint crack segmentation from individual classification

rithms have developed customized morphological transforms to solve this problem [28, 29] but they only work for very small discontinuities. One way to guide the expansion along the crack over large gaps is through tensor voting (TV) [30]. TV has been applied to connect disjointed crack segmentations as well [31, 32, 33, 34]. TV has been very effective in joining disjoint crack segments and eliminating noise. However, TV has two shortcomings. First, it is computationally expensive, making it infeasible for large-scale use or real-time processing. Secondly, it results in a blurred out image of the cracks which has to be further processed to obtain the final crack pattern.

Optimization approaches to crack detection work by modeling the crack detection problem as an optimization problem. This approach considers the assumption that cracks are long, continuous features. Also, by searching for an optimal solution, this approach has more robustness against changing crack widths and image quality. Huang and Tsai [35] used optimization for crack detection using local probability modeling and global probabilistic dynamic optimization [36]. This algorithm proved to be highly accurate but the computation required made it restrictive. Minimal-path-based algorithms attempt to detect cracks by searching for the optimal path across a potential map formed by the image, where a path along the crack provides the least resistance. Free-form anisotropy uses Djikstra's algorithm to find the lowest energy path around pixels (which lie on the crack) [8, 37], but interestingly discards this information in the final result. Amhaz et al. [38, 39] use Djikstra's

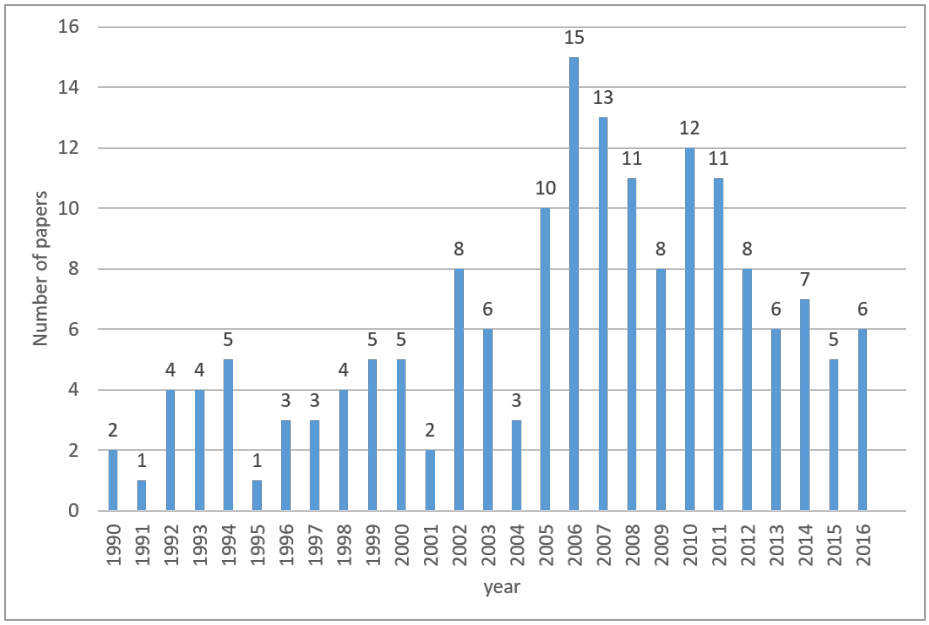

Figure 1.4: Number of papers on crack detection or classification published in a year

algorithm directly for crack detection by connecting a grid of points and then rejecting the unwanted linkages. This provides an accurate crack segmentation even in heavy noise, but several avenues of improvement remain to reduce the computational effort. Jiang [34] presented a minimal path based algorithm using the fast-marching method. The input points for the fast-marching method is provided by an individual classification step followed by tensor voting, skeletonization and endpoint detection. Minimal-path based methods clearly provide the most accurate yet robust results. However, the input points have to be provided, and the computation time of the current methods make them practically infeasible.

1.1.2 Trends in Crack Detection Research

Over 104 papers presenting crack detection methods were studied in this thesis. These papers were analyzed to gain insights on crack detection research trends. Figure 1.4 visualizes the publish date of papers related to crack detection and classification. An average of six papers have been published every year since 1990, underscoring the popularity of this problem.

The various common approaches to crack detection have already been explained in the

previous subsection. Let us formalize the approaches into four broad categories: Individual classification on the intensity/range image (IC-R); Individual classification on the frequency domain (IC-F); Individual classification followed by bottom-up approaches (BU); and Optimization (O). Table 1.1 lists the crack detection algorithms using each approach. Figure 1.5 visualizes the papers published on crack detection using each of the approaches. The size of the circles are proportional to the number of papers using that approach in that year. For a long time, crack detection algorithms focused on IC-R. Although IC-R is the most commonly used approach, its popularity has reduced in recent years. This does not mean individual classification on the intensity/range image is no longer used. It is still used for the preliminary crack segmentation in bottom-up and optimization based methods. IC-F has also become popular recently.

Table 1.1: Crack detection algorithm literature by approach

Approach	Papers
IC-R	[5, 9, 10, 12, 40, 41, 42, 43, 44, 45, 46, 47, 48, 49, 50, 51, 52, 53, 54, 55, 56, 57, 58, 59, 60, 61, 62, 63, 64, 65, 66, 67, 68, 69, 70, 71, 72, 73, 74]
IC-F	[14, 15, 18, 19, 20, 21, 22, 23, 24, 75, 76, 77, 78, 79, 80, 81, 82, 83, 84, 85, 86, 87, 88, 89, 90, 91]
BU	[26, 27, 28, 29, 31, 32, 33, 34, 92, 93, 94, 95, 96, 97, 98, 99, 100]
O	[8, 16, 35, 36, 37, 38, 39, 101, 102, 103, 104, 105, 106, 107, 108]
Other	[7, 109, 110]

1.2 Objectives and Scope

The objective of this thesis is to develop a fast and accurate crack detection algorithm. To achieve this objective, a minimal path based approach is targeted because of the high accuracy and robustness obtained. To address the issue of speed, a preliminary crack segmentation method using individual classification is proposed to limit the number of minimal path searches to only the crack pattern. To address the discontinuities in the crack pattern

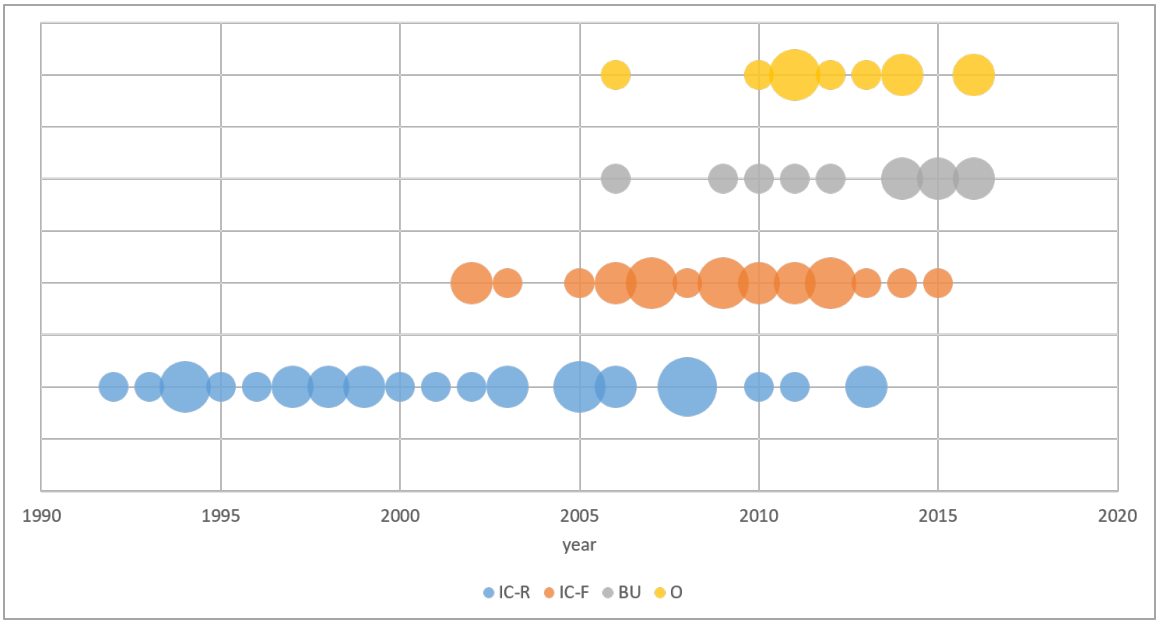

Figure 1.5: Papers published using different approaches to crack detection

due to the individual classification approach, a novel bottom-up method for connecting the disjoint crack pattern has been developed. The connected preliminary crack pattern will be used to generate the inputs for a minimal path algorithm, which will provide the final accurate crack segmentation. The Crack Detection Algorithm Performance Evaluation System (CDA-PES) has been used to evaluate the proposed algorithm and to compare it to the existing state-of-the-art algorithm.

CHAPTER 2
TECHNICAL APPROACH

The data collection procedure for the test pavement images is first described. The proposed algorithm has then been explained. Although the procedure has been optimized for the specific image format and size used in the data collection procedure, the procedure can be easily extended to other image formats and sizes after appropriate adjustment of some parameters.

2.1 Data Collection

Pavement image data is collected using the Georgia Tech Survey Vehicle (GTSV) shown in figure 2.1. Two laser scanners from Pavemetrics at the back of the vehicle collect intensity and range images of the pavement surface (figure 2.2). Intensity images have information on the brightness of the pavement surface. Range images contain information on the distance of the pavement surface from a fixed height. Cracks appear as sharp depressions on the pavement surface in the range image. Crack features are more clearly distinguishable in the range image. Thus, the range image is used for crack detection. Each pixel in the range image is a scalar value representing the depth of the pavement surface at that point. Lower values represent a lower depth. Rutting and the cross-slope of the pavement surface introduce a gradual change in the range value. This gradual change is removed by applying a Gaussian high-pass filter to the profiles. The range of values is scaled to fit between 0 and 255. These steps are completed at the image generation stage itself and are not considered part of the algorithm.

The sensors scan transverse profiles of the pavement at high speed. Each profile consists of 2,080 points spaced 1 mm apart. Combining both sensors gives a profile of 4,160 points spaced 1mm apart, covering 4.16 m (13.6 ft) in the transverse direction, which is enough

Figure 2.1: Georgia Tech Survey Vehicle (GTSV)

to cover one lane completely. The distance between consecutive profiles is 5 mm. Points are interpolated between the profiles to create additional profiles such that the distance between consecutive profiles reduces to 1mm. Therefore, a grid of points spaced 1mm apart in both the transverse and longitudinal directions is obtained. The information of every 5,000 profiles is encoded into an image. Each point of sensor data provides the information encoded in a pixel of a 4,160 by 5,000 pixel image.

2.2 Proposed Algorithm

The flowchart in figure 2.3 demonstrates the proposed algorithm. The major steps are as follows:

1. The image is preprocessed via median filtering to reduce noise.
2. A simplified individual classification algorithm is used to obtain a preliminary crack segmentation result.
3. Crack objects are generated and used to connect the disjoint crack segments and remove noise.
4. A minimal path based algorithm is used to detect the final crack pattern.

Each step is explained in detail in the subsections below.

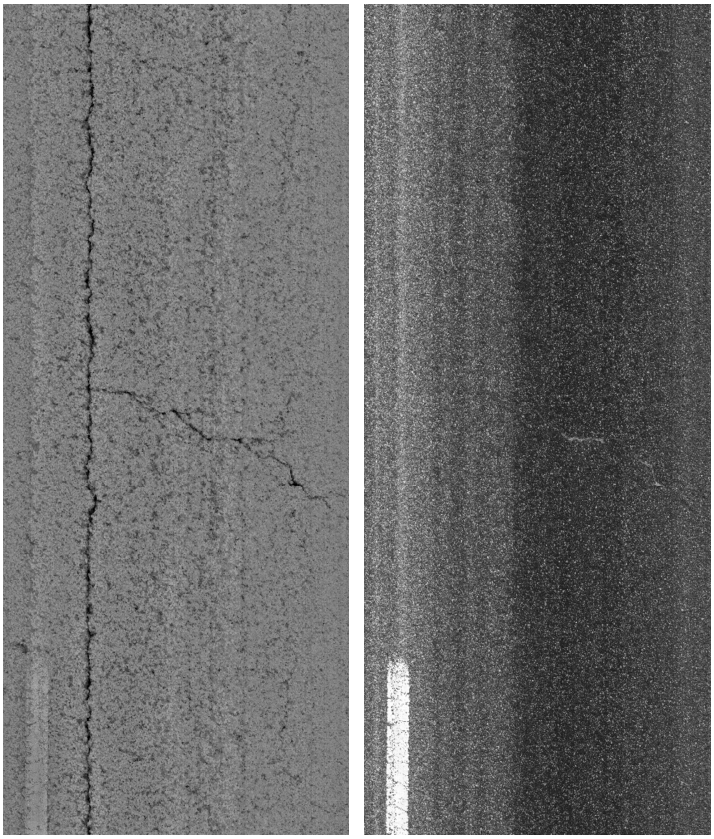

(a) Range Image (b) Intensity Image

Figure 2.2: Pavement images captured by 3D laser scanner on GTSV

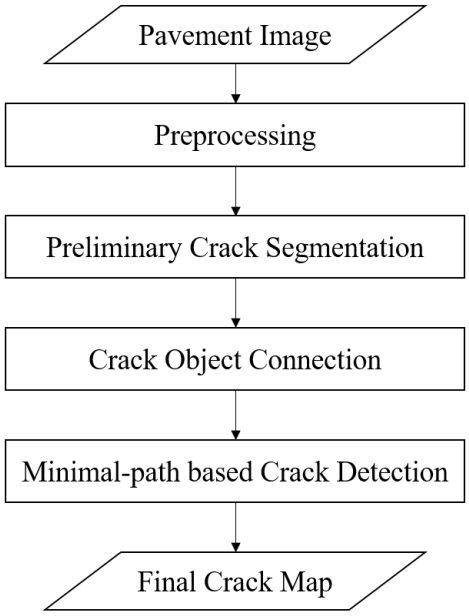

Figure 2.3: Proposed crack detection algorithm steps

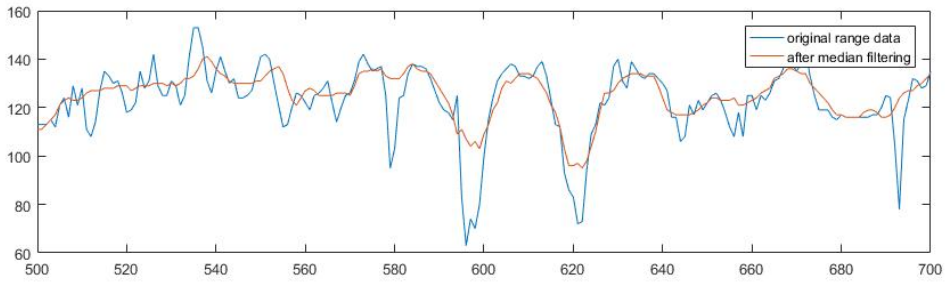

Figure 2.4: Effect of preprocessing

2.2.1 Preprocessing

As explained in section 2.1, the input image is a 4,160 by 5,000 pixel image with one channel: the range data. Some pixels may contain out-of-range values because of the pavement surface being outside the measurement range of the sensor or the presence of obstructions between the sensor and the pavement surface. In either case, these out-of-range values are outliers which produce a sharp gradient in the pavement image which can be mistaken for a crack. These pixels are however, almost always isolated and sparse. Therefore, a median blur is ideal for removing these outliers. A median blur with a window size of 9-by-9 pixels removes these outliers while preserving cracks. Figure 2.4 demonstrates the effect of the median blur.

2.2.2 Preliminary Crack Segmentation

A preliminary crack segmentation is carried out to remove the background. A simple thresholding is used to segment the crack pixels. It is difficult to determine an ideal global threshold that works for the entire image because of transverse undulations on the pavement surface caused by the camber and rutting. Hence, the image was divided into smaller subimages and an adaptive threshold was calculated for each subimage. To get the optimal size of the subimages, two constraints were taken into account.

1. The preliminary crack segmentation results were visibly inferior if the subimages represented a pavement width of more than 305 mm (1 foot). This was because the

aforementioned undulations made it difficult to define an ideal single threshold for the entire subimage.

2. The minimum subimage dimension had to be larger than the widest expected crack width, so that a subimage does not fall almost or completely inside a crack, making it difficult to find a suitable threshold from the subimage histogram. The widest cracks expected to be encountered are 51 mm (2 inches) wide.

The image was divided into 20×20 subimages. Thus, each subimage covered approximately 250 mm in the longitudinal direction and 200 mm in the transverse direction. As long as the number of subimages remained within the two constraints, there was no significant change in the preliminary crack segmentation. The computation speed is independent of the number of subimages.

Existing literature on crack detection using individual classification often did not mention the effect of different pavement types, as discussed in section 3.1.1. Open-Graded Friction Course (OGFC) Asphalt (Figure 3.2c) is extensively used in interstate highways in Georgia. However, its pavement texture, which clearly affects crack detection performance is generally not considered. A new adaptive threshold formula was required to encompass various pavement textures, including OGFC Asphalt surfaces, dense-graded asphalt surfaces and concrete surfaces [111]. Thus, a novel adaptive threshold formula was developed using the range image statistics, with the performance on various pavement textures taken into account.

Let S_i be the set of pixels in subimage i. The threshold is determined using the pixel value distribution of the subimage i as follows:

1. The mean and minimum value of the subimage i is determined.

$$v_{mean}^{(i)} = \frac{\sum_{j}^{j \in S_i} v_j}{|S_i|} \tag{2.1}$$

$$v_{min}^{(i)} = min_{j \in S_i} v_j \tag{2.2}$$

Where,

v_j is the range value of pixel j,

$v_{mean}^{(i)}$ is the mean range value of subimage i and

$min_{j \in S_i} v_j$ is the mean range value of subimage i

2. The threshold $t^{(i)}$ is then calculated using equation 2.3.

$$t^{(i)} = max(0, min(v_{min}^{(i)} + \alpha(v_{mean}^{(i)} - v_{min}^{(i)}) - \beta, \gamma)) \tag{2.3}$$

$$0 \leq \alpha \leq 1$$

$$\beta \geq 0$$

$$0 \leq \gamma \leq 255$$

Where α, β and γ are adjustable parameters. α controls the initial value of the threshold as a point between the mean and minimum range values of the subimage. For any non-zero value of α, there will be pixels which have a value below the threshold, even in subimages with no cracking. The pixel values of subimages with no cracking generally have less variance. The parameter β decreases the threshold slightly by a constant value. In case of subimages with no cracking, this slight shift pushes the threshold below the minimum value, preventing any pixels from being segmented as crack pixels. The parameter γ sets an upper limit for the threshold.

3. The preliminary crack segmentation map is generated. Pixels in S_i are classified as crack pixels if their range value i.e. depth is lower than $t^{(i)}$.

The parameters are adjusted to minimize the false negative error. This ensures that the thinner crack portions are not lost. This also results in a large number of false positives,

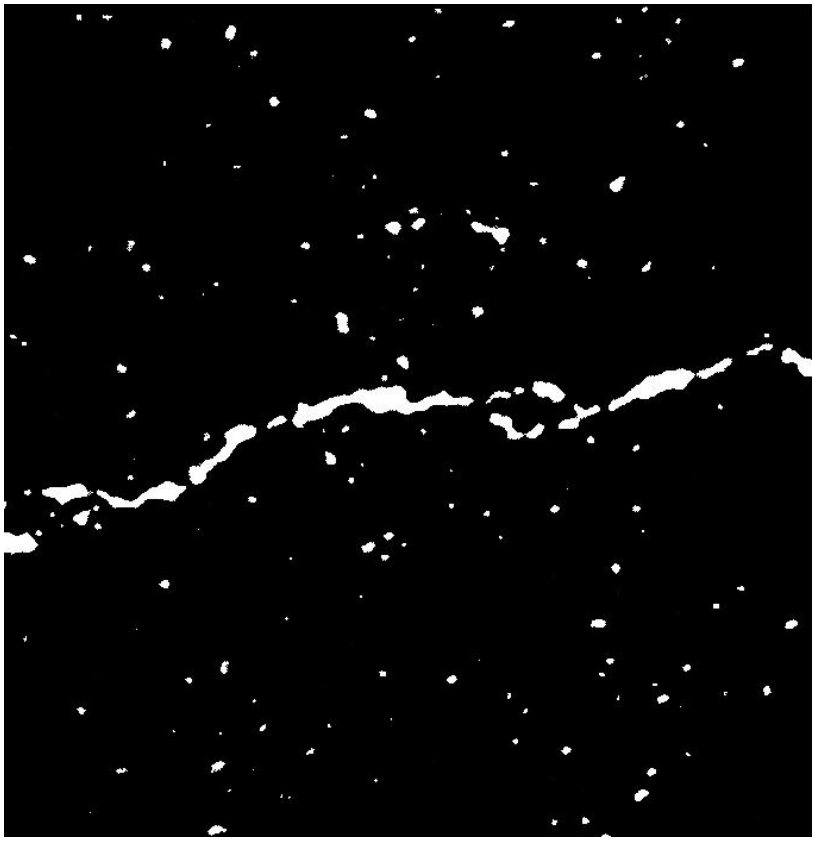

Figure 2.5: Result of preliminary crack segmentation

which are removed in the next step. The optimal parameters obtained by trial-and-error are given in table 2.1.

2.2.3 Crack Object Connection

A connected component is defined as a set of crack pixels such that every pixel in the set is connected to all other pixels through a path that passes exclusively through crack pixels through 8-neighbor connectivity. As shown in figure 2.5, connected components created from the true positive crack pixels (white) are generally more elongated and have an overall structure with a common local orientation. In contrast, connected components created from noise have no overall structure and no common orientation. These distinguishing properties are utilized to connect the crack features and remove the noise features.

1. Using the preliminary crack segmentation as the input, each connected component

having at least 10 pixels is used to create a crack object. Let R_i be the set of crack pixels in the preliminary crack segmentation that belong to crack object i. Then crack object i has the following properties:

(a) The Centroid ($C = (c_x, c_y)$) of the crack object is the centroid of the member crack pixels is given by equations

$$c_x = \mu_x = \frac{\sum_{j \in R_i} x_j}{|R_i|} \tag{2.4}$$

$$c_y = \mu_y = \frac{\sum_{j \in R_i} y_i}{|R_i|} \tag{2.5}$$

Where x_j and y_j are the x and y coordinates of pixel j respectively.

(b) The length (l) is equal to the variance along the first principal component of the pixels in R_i.

(c) The width (w) is equal to the variance along the second principal component of the pixels in R_i.

(d) The eccentricity (e) is given by equation 2.6.

$$e = \sqrt{1 - \frac{w^2}{l^2}} \tag{2.6}$$

The eccentricity varies between 0 and 1 and provides a measure of the elongation of the connected component. Larger values of eccentricity mean a more elongated shape and smaller values denote a rounder shape.

(e) The orientation (o) is given by the angle created by the principal component with the positive x-axis.

Figure 2.6 overlays the crack objects (magenta) over the preliminary crack segmentation (white). The crack objects are visualized as rectangles with the center, length,

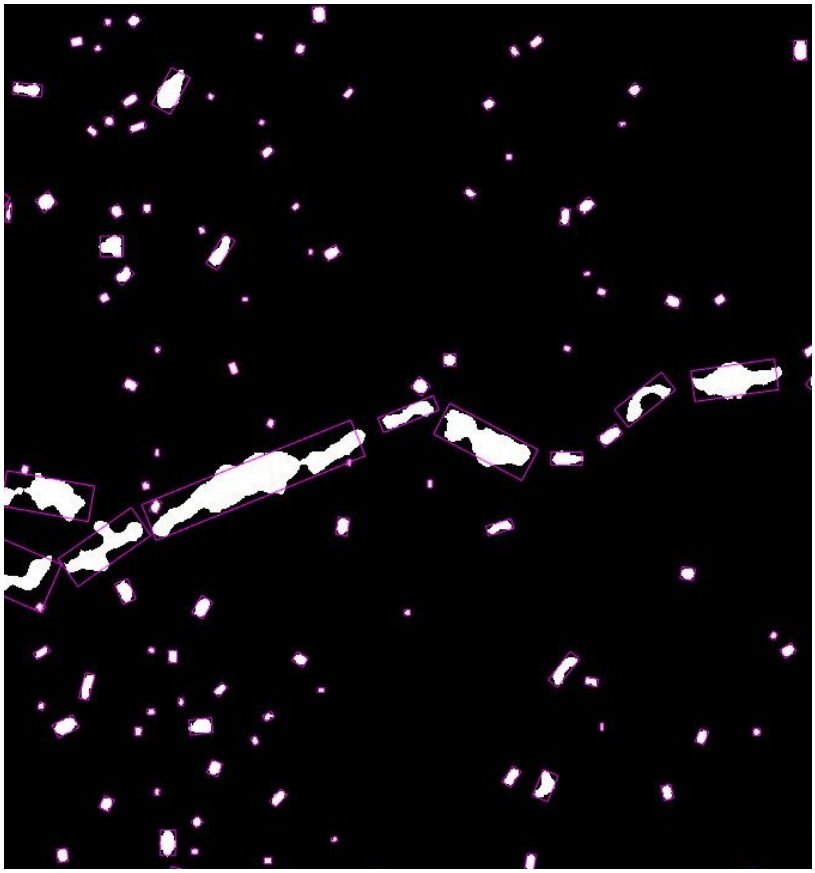

Figure 2.6: Crack objects overlay on preliminary image segmentation

width and angle of the length with the positive x-axis given by c, l, w and o of the crack object respectively.

2. Each crack object is elongated using equations 2.7 and 2.8.

$$l' = \mu l e^{\nu} \tag{2.7}$$

$$w' = w e^{\nu} \tag{2.8}$$

$$\mu, \nu > 1$$

Where l and l' are the initial and elongated lengths respectively,

w and w' are the initial and elongated widths respectively and

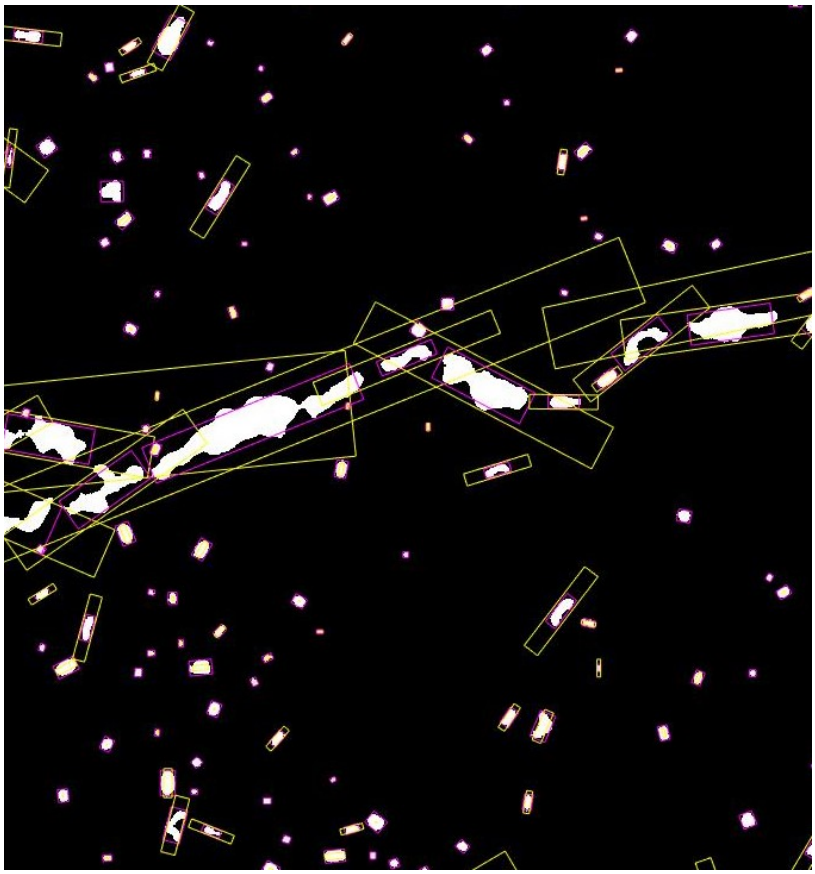

Figure 2.7: Elongated crack objects overlay on preliminary image segmentation

μ and ν are adjustable parameters

As we observed in figure 2.5, the crack objects created from the true positives are longer and more elongated. Hence, equations 2.7 and 2.8 were designed to incentivize crack objects that are longer and penalize noise which generally has low eccentricity. Figure 2.7 overlays the crack objects before (magenta) and after (yellow) elongation on the preliminary crack segmentation (white). The false positive crack objects are mostly shrunk down while the true positive crack objects are extended towards each other. The values for the parameters were determined by trial-and-error. The finalized parameter values are given in table 2.1.

3. Connected components analysis is then used to remove the false positive noise. The

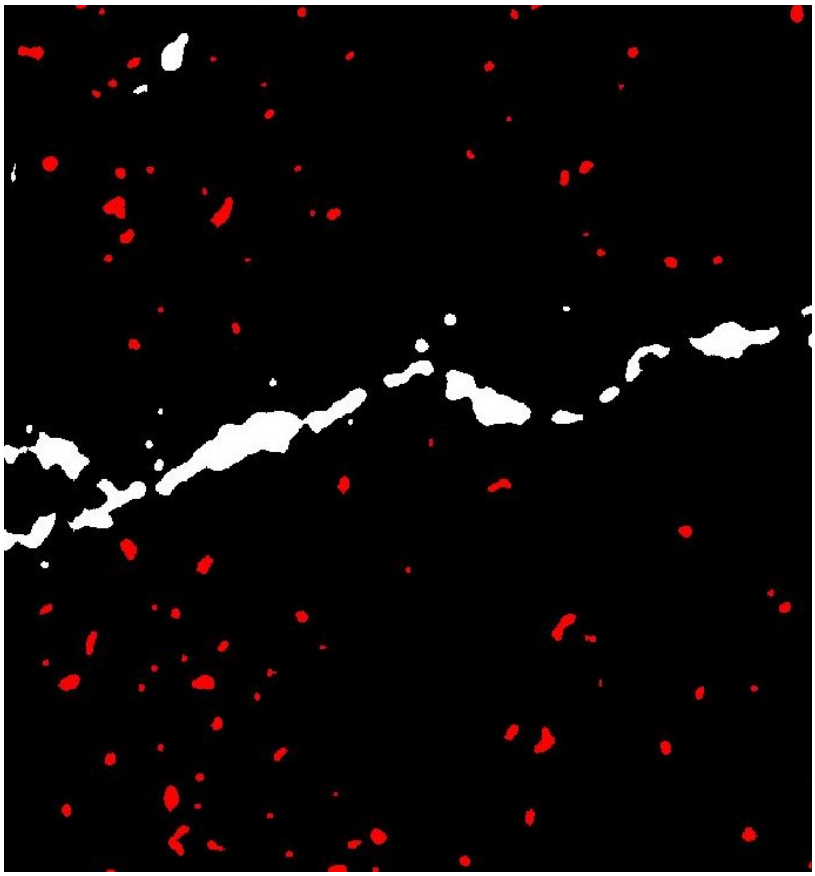

Figure 2.8: Removal of false positives

extended crack objects are used to calculate new connected components. For each crack object, a rectangle is drawn with the center of the rectangle coinciding with the centroid of the crack object. The length, width and the angle made by the length of the rectangle with the positive x-axis are given by l', w' and o respectively. Rectangles that overlap would belong to the same connected component. The isolated false positive connected components are much smaller than the true positive connected components which are connected together. This image of overlaid crack object rectangles is skeletonized and connected components of size smaller than the parameter δ are removed. This eliminates the false positive noise from the image, leaving only the interconnected crack pattern intact. The optimal value of parameter δ was determined by trial-and-error and is given in table 2.1. Figure 2.8 visualizes the removed crack objects (red) and the remaining crack objects (white).

Table 2.1: Parameter values

Parameter	Value
α	0.85
β	10
γ	65
δ	10
μ	2.7
ν	1.5

2.2.4 Minimal Path Crack Detection

From the previous subsection, a crack segmentation map is obtained with most false positives and false negatives removed and the disjoint crack segments patched together. Minimal Path detection using the fast-marching algorithm was used to refine this image using the following steps.

1. The branchpoints of the image were identified. These branchpoints along with their neighboring pixels set to zero in the refined crack segmentation. As a result, the image would be left with curves with no branching.

2. The endpoints of the each curve are then identified. These endpoints serve as the input points for the fast-marching algorithm.

3. The fast-marching algorithm is used to find an optimal path between each pair of points using the original range image as the potential map. The minimal path falls along the crack pixels, which have greater depth than the surrounding pavement, hence lower weight associated with them.

4. Finally, the detected paths are filtered according to the following criteria:

   (a) Paths less than 20 pixels long (corresponding to approximately 20mm length) are rejected. This is done to remove artifacts developed from the skeletonization step which leaves small spurs on the skeleton.

(b) Paths with a mean pixel value greater than the mean value of the entire image are rejected. Paths along cracks are expected to have lower mean values than the rest of the image. This step removes erroneous paths.

5. The removed branchpoints are added back, connecting the minimal path curves.

2.3 Demonstration

Figures 2.9 and 2.10 demonstrate the proposed algorithm on two pavement images. Figure 2.9 has been explained in detail. The same logic applies for figure 2.10 as well.

Figure 2.9a shows the original range image. Figure 2.9b shows the result of the preliminary crack segmentation. Small false positive noise can be seen scattered throughout the image by design. The crack is also represented as small connected components, but these connected components are generally elongated along the crack to form an overall pattern. As a result, the crack objects formed by these connected components are extended along the same direction and are joined, as shown in figure 2.9c. On the other hand, the false positive noise connected components remain isolated because they have little extension and arbitrary orientation. Figure 2.9d shows the result after the patched image is skeletonized and the small connected components have been removed. The endpoints and branchpoints of this image are then used as inputs for a minimal path search algorithm. The results of the minimal path search are shown overlaid on the original image in figure 2.9e. After filtering the minimal paths, the final crack segmentation is shown in figure 2.9f. The effect of the final filtering can be better observed in figure 2.10e and 2.10f.

The final crack segmentation is a connected crack pattern with minimal false positive noise. Even thin cracks are detected, minimizing false negatives. Figure 2.10 shows a challenging case where the proposed algorithm missed some crack segments, indicating avenues for future improvement.

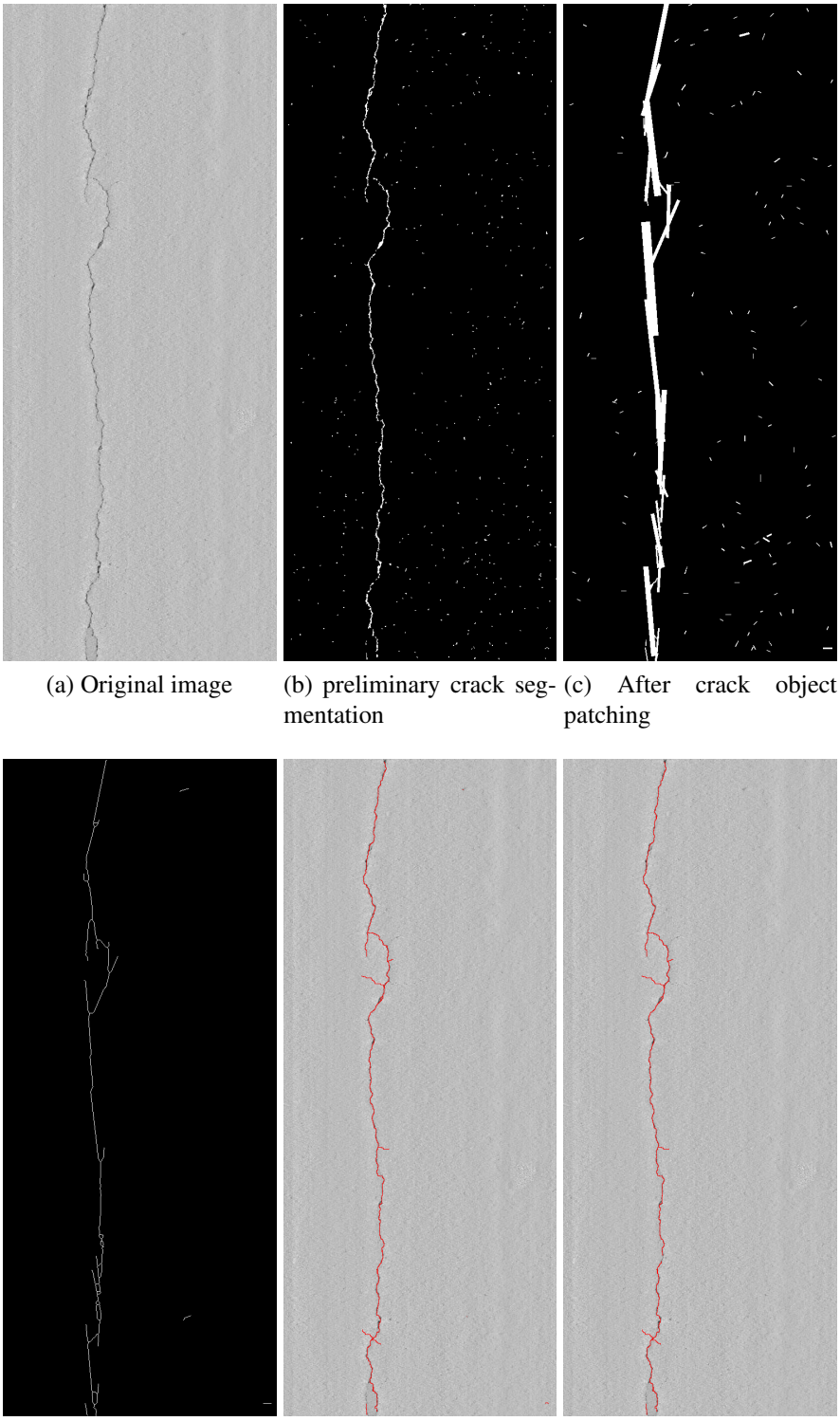

(a) Original image (b) preliminary crack segmentation (c) After crack object patching

(d) Skeletonized image (e) After minimal path search (f) Final crack segmentation

Figure 2.9: Demonstration of proposed algorithm on image with longitudinal crack

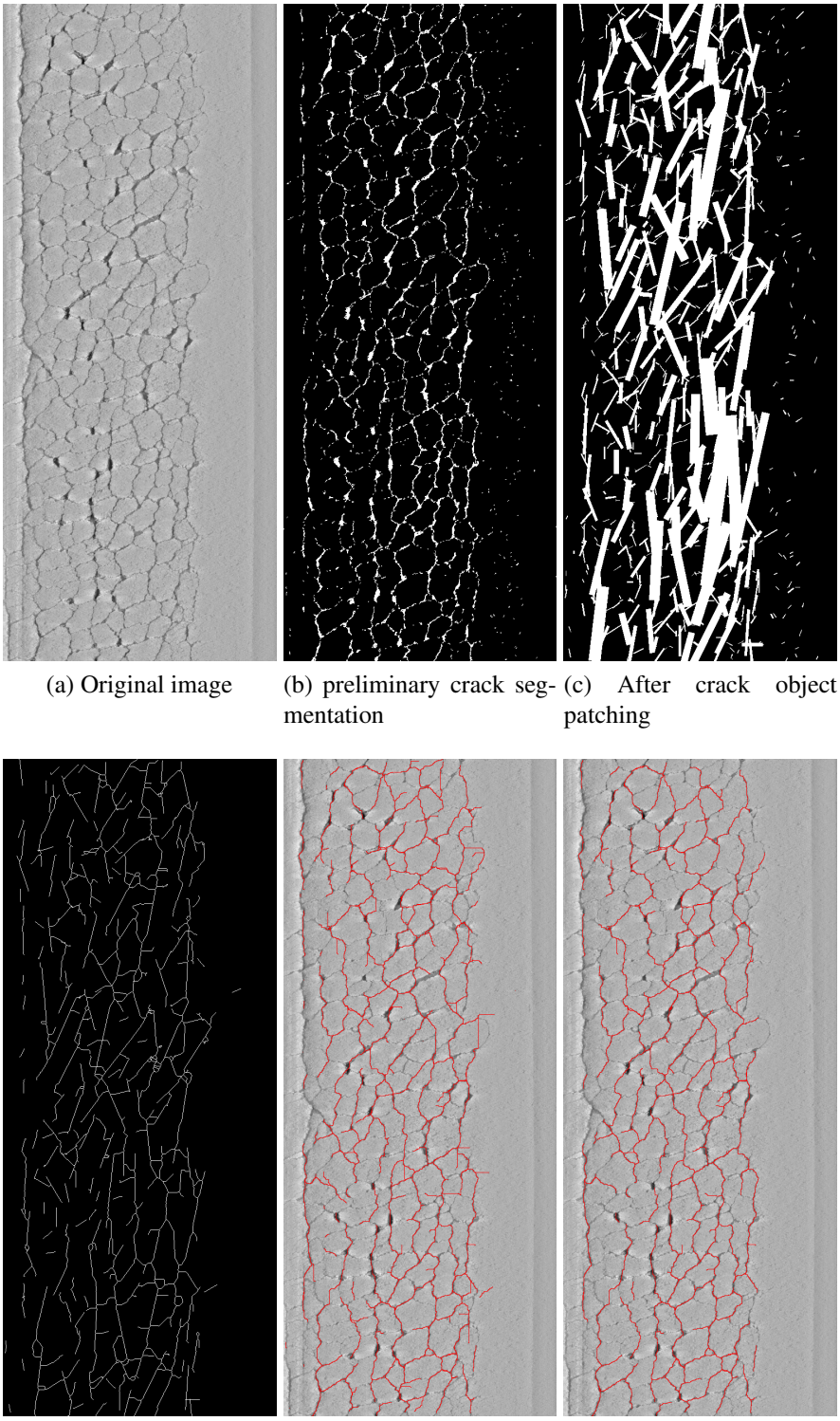

(a) Original image (b) preliminary crack segmentation (c) After crack object patching

(d) Skeletonized image (e) After minimal path search (f) Final crack segmentation

Figure 2.10: Demonstration of proposed algorithm on image with longitudinal crack

CHAPTER 3

RESULTS

Rigorous performance evaluation and comparative analysis was performed on the proposed algorithm. This chapter presents the tests conducted and the results achieved. The tests were conducted on a machine with an Intel Core i7-4770 CPU 8 cores @ 3.40GHz. The results show superior performance by the proposed algorithm on the Crack Detection Algorithm - Performance Evaluation System (CDA-PES) [111] as compared to all algorithms tested before on CDA-PES. The proposed algorithm also shows much lower computation time as compared to the state-of-the-art algorithm by Jiang [34], the only other algorithm to achieve comparable performance in the CDA-PES.

3.1 Accuracy

This section considers the correctness of the crack detection results obtained by the proposed algorithm. The Crack Detection Algorithm - Performance Evaluation System (CDA-PES) has been used for evaluation. Section 3.1.1 summarizes the CDA-PES. The performance result of the proposed algorithm in CDA-PES is given in section 3.1.2. This is followed by a comparison with existing algorithms in section 3.1.3.

3.1.1 Crack Detection Algorithm - Performance Evaluation System (CDA-PES)

The CDA-PES consists of:

1. An enhanced Hausdorff distance-based quantitative performance evaluation metric.
2. A consistent dataset designed with diverse pavement types and crack conditions that affect CDA performance.

3. A multi-level, categorized, quantitative performance scoring and reporting method to critically assess the CDA performance and provide feedback to researchers.

The performance metric is used to evaluate the performance of a crack detection algorithm on a pavement image. It is used on all images in the pavement image dataset to obtain a detailed performance evaluation of the algorithm, which is visualized using the provided scoring and reporting method.

Performance Metric

Commonly, crack detection is treated as a binary classification problem: each pixel has to be individually classified as a ”crack pixel” or a ”non-crack pixel”. Hence, binary classifier metrics such as accuracy, precision and recall are often used to evaluate crack detection algorithms. However, classifying pixels in an image as a ”crack pixel” or a ”non-crack pixel” is subjective [111].

To overcome this problem of subjectivity, an enhanced Hausdorff distance-based performance metric is used. In this metric, a no-penalty buffer is created around the ground truth crack segmentation. The ground truth crack segmentation is created once manually. Any crack pixels detected inside this buffer will not receive any penalty. As the distance of crack pixels grow farther away from the ground truth, the penalty starts to rise until the maximum penalty is alloted. As a result, false positive crack pixels are penalized. Next, the same buffer is drawn along the detected crack pattern and crack pixels in the ground truth which are outside this buffer receive a penalty. This way, false negatives are also penalized.

Combining the penalties of the two images provides a final score out of 100 for the performance of a crack detection algorithm on a particular image. Higher scores indicate better performance. The regions of the image which caused the false positive or false negatives can be easily identified, providing a more detailed visualization of the performance.

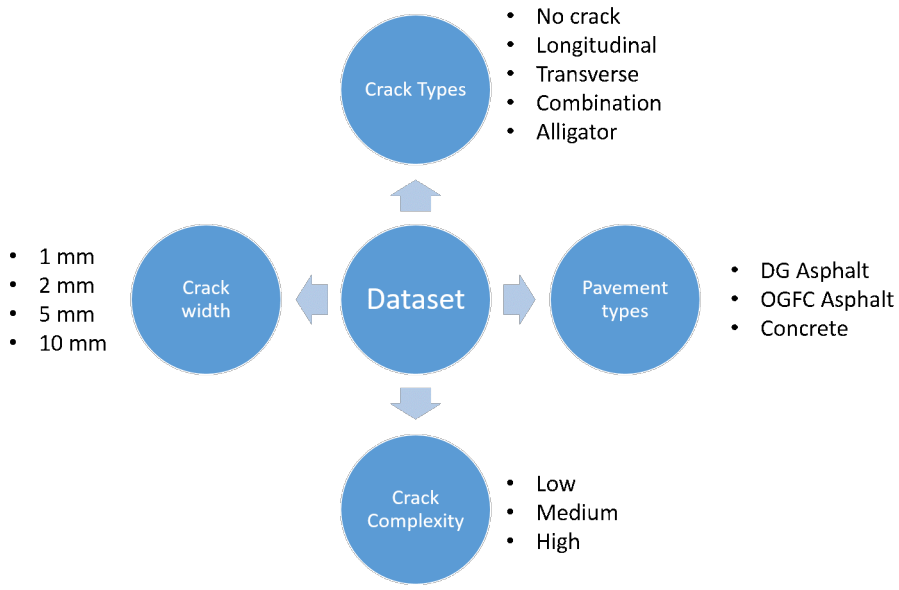

Figure 3.1: Categories in the CDA-PES pavement image dataset

Pavement Image Dataset

The factors affecting crack detection algorithms were considered during the development of the pavement image dataset in CDA-PES. The four factors considered were pavement type, crack type, crack width and crack complexity (Figure 3.1).

- Pavement type drastically changes the appearance of the pavement surface. Figure 3.2 shows the difference between three pavement types and their effect on a thresholding-based crack detection algorithm.

- Crack type refers to the different cracking conditions that can be found on pavement surfaces. Figure 3.3 shows some of the images from the dataset representing different cracking conditions.

- Crack width often affects crack detection performance. However, cracks generally have different widths throughout their structure. To capture the effect of different crack widths on crack detection performance, synthetic images were created. Figure 3.4 show these synthetic images and their effect on an edge detection based algorithm.

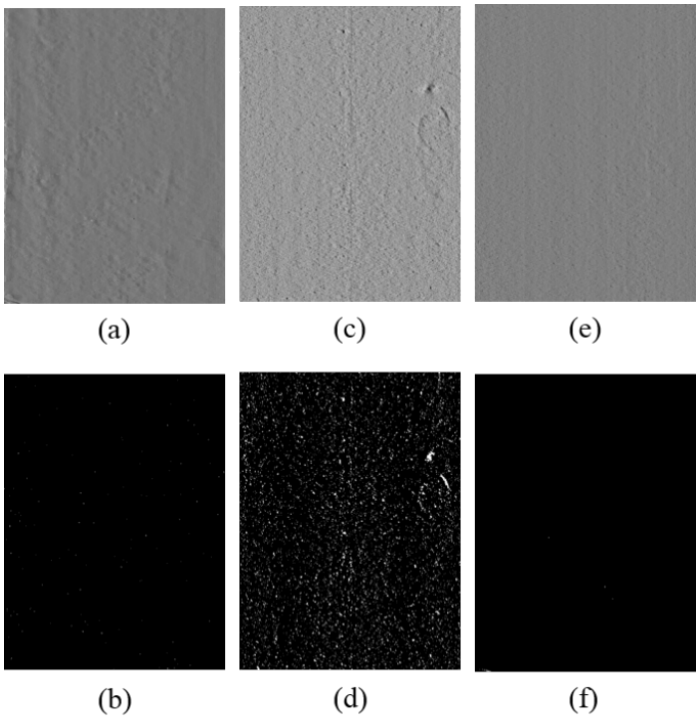

Figure 3.2: Different pavement types: (a) Dense graded asphalt pavement range image; (b) Crack map detected by relaxation thresholding on Figure 3.2a; (c) open graded friction course asphalt pavement range image; (d) Crack map detected by relaxation thresholding on Figure 3.2c; (e) Concrete pavement; (f) Crack map detected by relaxation thresholding on Figure 3.2e

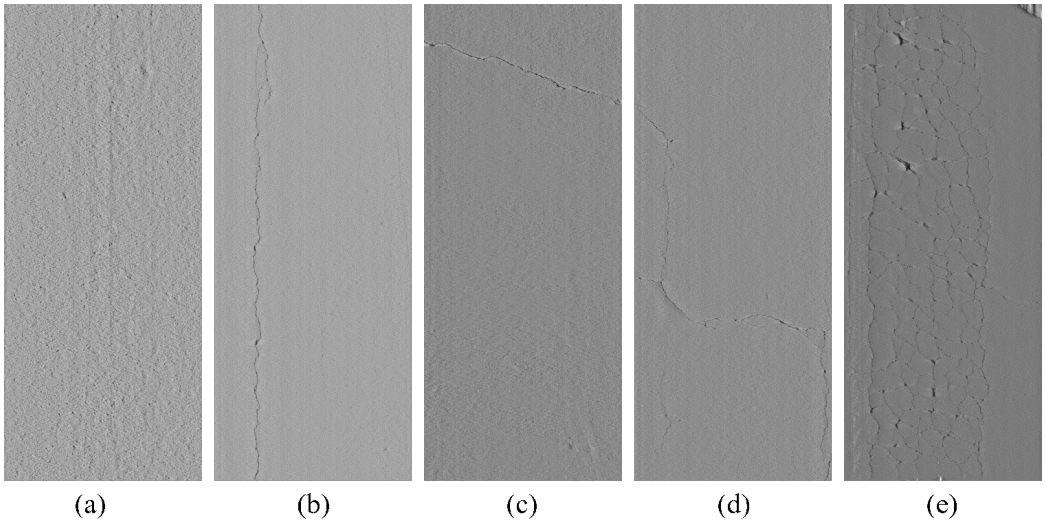

Figure 3.3: Different crack types: (a) no cracking; (b) longitudinal crack; (c) transverse crack; (d) combination of crack types; (d) alligator cracking

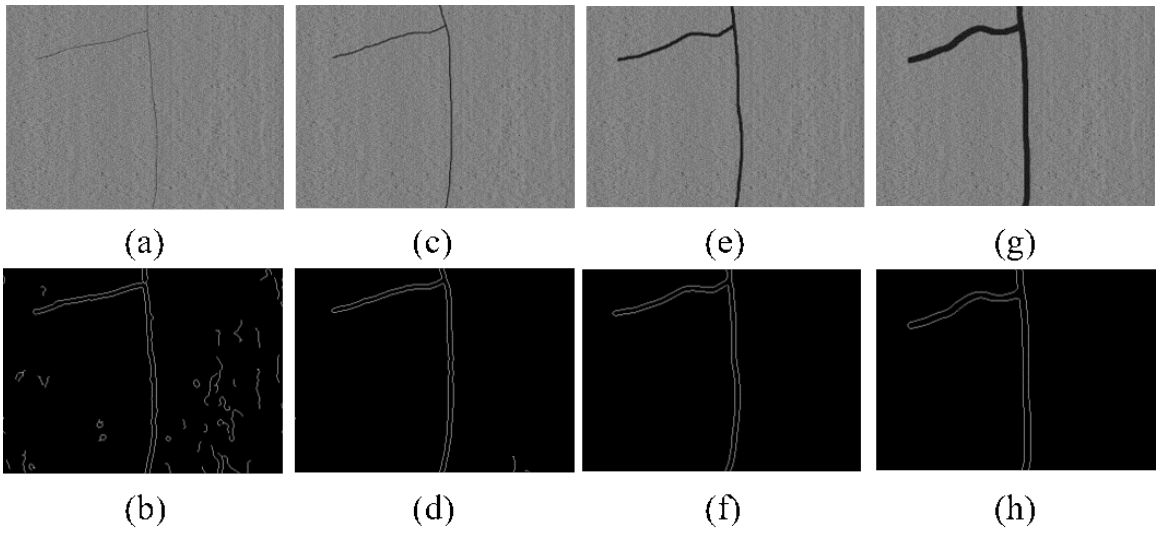

Figure 3.4: Different crack widths: (a) 1 pixel crack width; (b) Canny edge detection result on Fig 3.4a; (c) 2 pixel crack width; (d) Canny edge detection result on fig 3.4c; (e) 5 pixel crack width; (f) Canny edge detection on Fig 3.4e; (g) 10 pixel crack width; (h) Canny edge detection on Fig 3.4g

- The number of intersecting points and polygons in a crack image affects some crack detection algorithms' accuracy as well as computation speed. Figure 3.5 demonstrates images with different crack complexities.

Scoring and Reporting

CDA-PES provides three levels of performance evaluation of crack detection algorithms. The first level is an overall score for the algorithm, with 100 being the highest score that

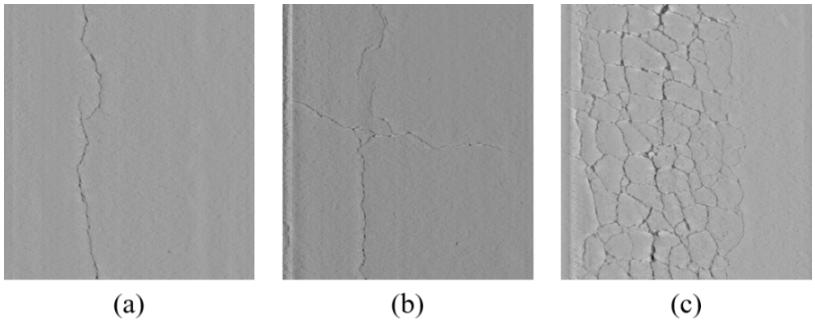

Figure 3.5: Different crack complexities: (a) low pattern complexity; (b) medium pattern complexity; (c) high pattern complexity

can be achieved. The second level is a set of scores for various image subsets, which helps to identify the weaknesses of CDAs. This is visualized in a CDA-PES dashboard (figure 3.6). The third level provides individual image scores and visualizations of the source of penalties. This helps to identify the cause of penalties, helping to improve the CDA.

3.1.2 CDA-PES Results

Figure 3.6 shows the CDA-PES dashboard for the proposed algorithm. The overall score is 80, the highest ever recorded using the CDA-PES [111].

The weakest category appeared to be transverse cracks, which are often difficult to detect because of their thin widths. Alligator cracking also pulled the overall score down. In both cases, the reason was mainly false negative error, propagated by thin cracks. These categories show the area for future improvement for the proposed algorithm. The performance is not significantly affected by crack width although it appears to clearly decline as crack complexity increases.

3.1.3 Comparison to existing algorithms

The tensor voting based MPS algorithm (further refered to as the TV algorithm) presented by Jiang [34] has been considered the state-of-the-art algorithm for this comparative analysis. Table 3.1 shows the overall CDA-PES scores obtained by various existing algorithms, the TV algorithm and the proposed algorithm. The TV algorithm and the proposed algorithm have the highest overall scores.

Figure 3.7 shows the CDA-PES dashboard for the TV algorithm. It can be observed that the TV algorithm has lower false positives, but slightly higher false negative errors. Both algorithms are minimal-path based. Thus, they both have difficulty in complex crack patterns such as alligator cracking and easily remove noise in images with no cracking. The proposed algorithm performs better in all categories with cracking.

Figure 3.6: Dashboard for proposed algorithm

Figure 3.7: Dashboard for tensor voting based MPS algorithm [34]

Table 3.1: Comparison of overall CDA-PES scores [111]

Crack Detection Algorithm	Overall Score
Relaxation Thresholding	63
Canny Edge Detection	48
Wavelet-based Detection	28
Iterative Clipping	28
Seed-based Method	50
Dynamic Optimization	71
Tensor voting based MPA	79
Proposed algorithm	80

3.2 Computation Speed

The greatest advantage of the proposed algorithm with respect to the state-of-the-art algorithm is a vast reduction in computation time. This is mainly attributed to the novel approach to connect disjoint crack segments which replaces the computationally heavy tensor voting step. The computation speed for processing the CDA-PES pavement image dataset has been considered. The dataset consists of 68 images of size 0.65 megapixels.

3.2.1 Computation Time Breakdown

The proposed algorithm has a minimal path search step. The computation time for the minimal path search step varies greatly as the complexity of the crack pattern changes. Figure 3.8 shows the computation time of the proposed algorithm on three separate images with varying crack complexity. The minimal path search step clearly becomes the most computationally heavy step in the algorithm for images with cracks.

The proposed algorithm was used to process 68 images in the CDA-PES pavement image dataset. The proposed algorithm took on average 1.15 seconds per image. The distribution of processing times (figure 3.9) shows that this is a skewed distribution. The median computation time is 0.52 seconds.

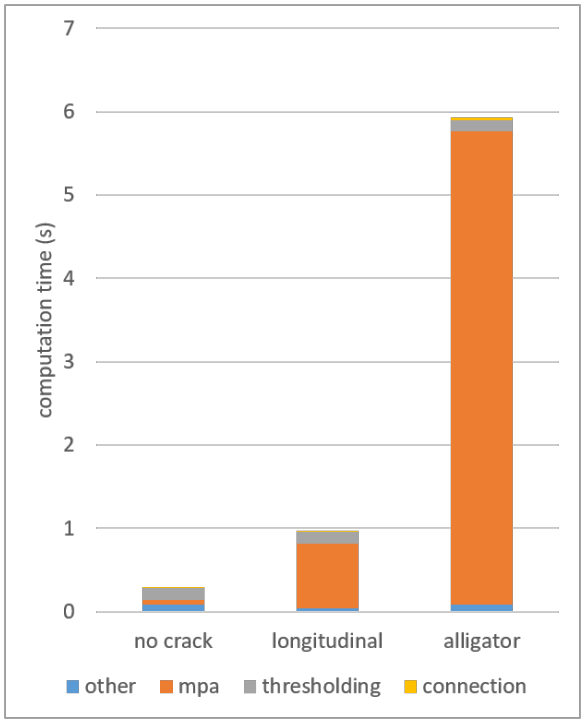

Figure 3.8: Computation time of proposed algorithm

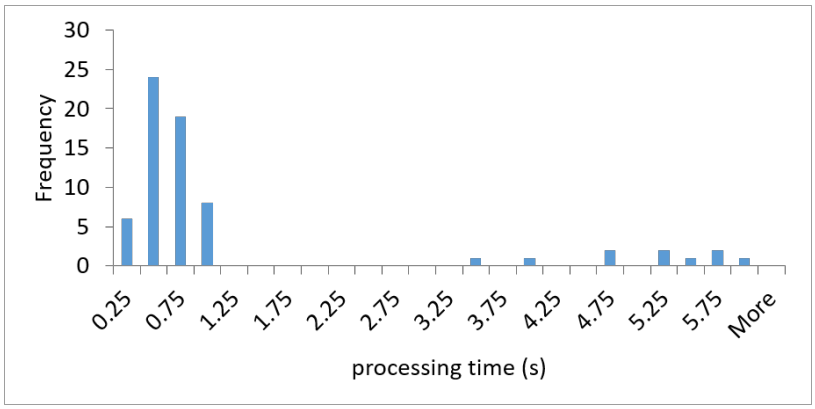

Figure 3.9: Distribution of computation time of proposed algorithm

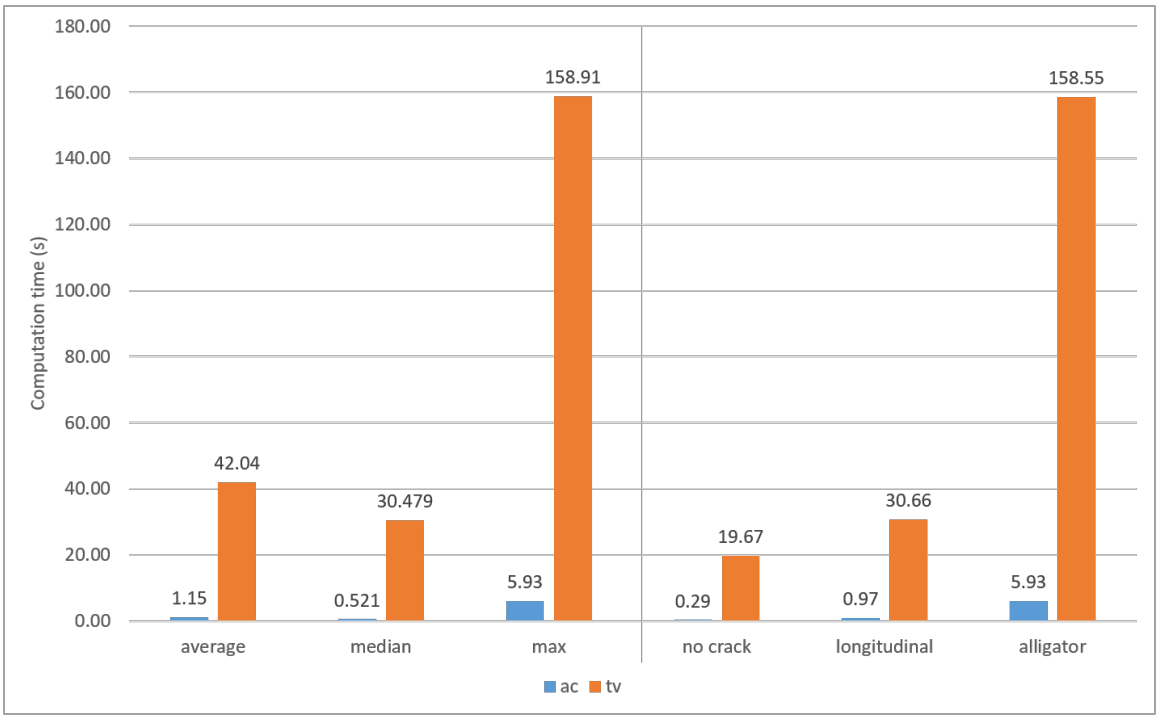

Figure 3.10: Comparison of computation time

3.2.2 Comparison with the state of the art

Figure 3.10 demonstrates the speed improvement over the current state-of-the-art TV algorithm. The proposed algorithm has a 36 times faster average computation speed and a 58 times faster median computation speed. When compared on the same image, the proposed algorithm performed 68, 32 and 27 times faster in an image with no cracking, one longitudinal crack and alligator cracking respectively.

CHAPTER 4
CONCLUSION

4.1 Contributions

This thesis presented a fast and accurate crack detection algorithm. The core contribution to crack detection research is a novel preliminary crack segmentation method and a fast method for connecting the disjoint crack pattern as an alternative to tensor voting. These contributions provide a method to automatically obtain the input points for the fast-marching algorithm, which has been found to be very accurate in finding the crack path between between two given points on a crack.

The algorithm presented in this thesis offers a robust, accurate and fast crack detection algorithm which will have a strong beneficial impact on the widespread adoption of automated road condition surveys, making road condition surveys safer and more efficient.

4.2 Future Recommendations

1. The proposed algorithm achieves better overall performance. However, potential for improvement remains, especially in the case of high crack complexity. From figure 2.10, the problem appears to be ”overpatching”, where the patched image appears to lose information about the crack topology. Further research is required to improve the performance in this category.

    (a) One possible approach is to detect cases of alligator cracking and reduce the elongation parameters μ and ν, which can possibly improve the performance in the case of images with high crack complexity.

    (b) An alternative solution is to detect image regions of alligator cracking (image blocks with a large number of crack pixels during the preliminary crack seg-

mentation) and stop any further analysis in those regions, which can be done by setting all pixels in those regions as non-crack pixels. The alligator cracking region can then be delivered as a second output, represented with just a bounding box. This secondary output format is sufficient for the purposes of road condition surveys, in which alligator cracking is generally recorded as the overall pavement length/area affected, not the exact crack pattern.

2. Another difficult category was transverse cracking, which generally has very thin cracks. Further research has to be conducted to preserve these transverse cracks.

3. Although significant speed improvements have been achieved, the proposed algorithm cannot be directly applied in real-time. Parallel and GPU processing is recommended to further improve the speed of the algorithm. The minimal path search step was found to be the heaviest step in the algorithm, especially in the case of high crack complexity. Each minimal path search is independent of the others. Hence, the algorithm can greatly benefit from parallelization.

4. The application of the proposed crack detection algorithm in other fields can be explored. Crack detection has applications in bridge inspection, building information modeling, manufacturing and medical imaging.

5. The crack objects already store useful information about the crack pattern. This crack pattern information can have applications in crack classification. The possibility of using the crack object data for crack classification should be explored.

REFERENCES

[1] FHWA, "Status of the federal highway trust fund 1957-2015," Federal Highway Administration, Tech. Rep. FE-210C, 2015.

[2] S. Chambon and J.-M. Moliard, "Automatic road pavement assessment with image processing: Review and comparison," *International Journal of Geophysics*, vol. 2011, 2011.

[3] GDOT, "Pavement condition evaluation system," Georgia Department of Transportation, Tech. Rep., 2007.

[4] H. N. Koutsopoulos, I. E. Sanhouri, and A. B. Downey, "Analysis of segmentation algorithms for pavement distress images," *Journal of transportation engineering*, vol. 119, no. 6, pp. 868–888, 1993.

[5] Y. Huang and B. Xu, "Automatic inspection of pavement cracking distress," *Journal of Electronic Imaging*, vol. 15, no. 1, pp. 013 017–013 017, 2006.

[6] B. J. Lee, H. Lee, *et al.*, "Position-invariant neural network for digital pavement crack analysis," *Computer-Aided Civil and Infrastructure Engineering*, vol. 19, no. 2, pp. 105–118, 2004.

[7] F Roli, "Measure of texture anisotropy for crack detection on textured surfaces," *Electronics Letters*, vol. 32, no. 14, pp. 1274–1275, 1996.

[8] T. S. Nguyen, S. Begot, F. Duculty, and M. Avila, "Free-form anisotropy: A new method for crack detection on pavement surface images," in *Image Processing (ICIP), 2011 18th IEEE International Conference on*, IEEE, 2011, pp. 1069–1072.

[9] H Cheng, J. Wang, Y Hu, C Glazier, X Shi, and X Chen, "Novel approach to pavement cracking detection based on neural network," *Transportation Research Record: Journal of the Transportation Research Board*, no. 1764, pp. 119–127, 2001.

[10] H.-D. Cheng, "Automated real-time pavement distress detection using fuzzy logic and neural network," in *Nondestructive Evaluation Techniques for Aging Infrastructure and Manufacturing*, International Society for Optics and Photonics, 1996, pp. 140–151.

[11] V. Badrinarayanan, A. Kendall, and R. Cipolla, "Segnet: A deep convolutional encoder-decoder architecture for image segmentation," *ArXiv preprint arXiv:1511.00561*, 2015.

[12] S. J. Schmugge, L. Rice, J. Lindberg, R. Grizziy, C. Joffey, and M. C. Shin, "Crack segmentation by leveraging multiple frames of varying illumination," in *Applications of Computer Vision (WACV), 2017 IEEE Winter Conference on*, IEEE, 2017, pp. 1045–1053.

[13] J. Canny, "A computational approach to edge detection," *IEEE Transactions on pattern analysis and machine intelligence*, no. 6, pp. 679–698, 1986.

[14] H. Zhao, G. Qin, and X. Wang, "Improvement of canny algorithm based on pavement edge detection," in *Image and Signal Processing (CISP), 2010 3rd International Congress on*, IEEE, vol. 2, 2010, pp. 964–967.

[15] A Cubero-Fernandez, F. J. Rodriguez-Lozano, R. Villatoro, J. Olivares, and J. M. Palomares, "Efficient pavement crack detection and classification," *EURASIP Journal on Image and Video Processing*, vol. 2017, no. 1, p. 39, 2017.

[16] G. Li, X. Zhao, K. Du, F. Ru, and Y. Zhang, "Recognition and evaluation of bridge cracks with modified active contour model and greedy search-based support vector machine," *Automation in Construction*, vol. 78, pp. 51–61, 2017.

[17] S. Mallat and S. Zhong, "Characterization of signals from multiscale edges," *IEEE Transactions on pattern analysis and machine intelligence*, vol. 14, no. 7, pp. 710–732, 1992.

[18] A Cuhadar, K Shalaby, and S Tasdoken, "Automatic segmentation of pavement condition data using wavelet transform," in *Electrical and Computer Engineering, 2002. IEEE CCECE 2002. Canadian Conference on*, IEEE, vol. 2, 2002, pp. 1009–1014.

[19] J. Zhou, P. Huang, and F.-P. Chiang, "Wavelet-based pavement distress classification," *Transportation Research Record: Journal of the Transportation Research Board*, no. 1940, pp. 89–98, 2005.

[20] J. Zhou, P. S. Huang, and F.-P. Chiang, "Wavelet-based pavement distress detection and evaluation," *Optical Engineering*, vol. 45, no. 2, pp. 027 007–027 007, 2006.

[21] P. Subirats, J. Dumoulin, V. Legeay, and D. Barba, "Automation of pavement surface crack detection using the continuous wavelet transform," in *Image Processing, 2006 IEEE International Conference on*, IEEE, 2006, pp. 3037–3040.

[22] K. Wang, Q. Li, and W. Gong, "Wavelet-based pavement distress image edge detection with a trous algorithm," *Transportation Research Record: Journal of the Transportation Research Board*, no. 2024, pp. 73–81, 2008.

[23] S. Chambon, P. Subirats, and J. Dumoulin, "Introduction of a wavelet transform based on 2d matched filter in a markov random field for fine structure extraction: Application on road crack detection," in *IS&T/SPIE Electronic Imaging*, International Society for Optics and Photonics, 2009, 72510A–72510A.

[24] B. Sun and Y. Qiu, "Automatic pavement surface cracking recognition using wavelet transforms technology," in *International Conference on Transportation Engineering 2009*, 2009, pp. 2201–2206.

[25] J. Serra, "Introduction to mathematical morphology," *Computer vision, graphics, and image processing*, vol. 35, no. 3, pp. 283–305, 1986.

[26] K. C. Wang and W. Gong, "Real-time automated survey system of pavement cracking in parallel environment," *Journal of infrastructure systems*, vol. 11, no. 3, pp. 154–164, 2005.

[27] E Salari and G Bao, "Pavement distress detection and classification using feature mapping," in *Electro/Information Technology (EIT), 2010 IEEE International Conference on*, IEEE, 2010, pp. 1–5.

[28] D. Zhang, Q. Li, Y. Chen, M. Cao, L. He, and B. Zhang, "An efficient and reliable coarse-to-fine approach for asphalt pavement crack detection," *Image and Vision Computing*, vol. 57, pp. 130–146, 2017.

[29] A. Zhang, K. C. Wang, R. Ji, and Q. J. Li, "Efficient system of cracking-detection algorithms with 1-mm 3d-surface models and performance measures," *Journal of Computing in Civil Engineering*, vol. 30, no. 6, p. 04 016 020, 2016.

[30] G. Medioni, C.-K. Tang, and M.-S. Lee, "Tensor voting: Theory and applications," in *Proceedings of RFIA*, vol. 2000, 2000.

[31] Q. Zou, Y. Cao, Q. Li, Q. Mao, and S. Wang, "Cracktree: Automatic crack detection from pavement images," *Pattern Recognition Letters*, vol. 33, no. 3, pp. 227–238, 2012.

[32] J. Huang, W. Liu, and X. Sun, "A pavement crack detection method combining 2d with 3d information based on dempster-shafer theory," *Computer-Aided Civil and Infrastructure Engineering*, vol. 29, no. 4, pp. 299–313, 2014.

[33] H. Guan, J. Li, Y. Yu, M. Chapman, H. Wang, C. Wang, and R. Zhai, "Iterative tensor voting for pavement crack extraction using mobile laser scanning data," *IEEE*

Transactions on Geoscience and Remote Sensing, vol. 53, no. 3, pp. 1527–1537, 2015.

[34] C. Jiang, "A crack detection and diagnosis methodology for automated pavement condition evaluation," PhD thesis, Georgia Institute of Technology, 2015.

[35] Y. Huang and Y. Tsai, "Dynamic programming and connected component analysis for an enhanced pavement distress segmentation algorithm," *Transportation Research Record: Journal of the Transportation Research Board*, no. 2225, pp. 89–98, 2011.

[36] O. Alekseychuk, "Detection of crack-like indications in digital radiography by global optimisation of a probabilistic estimation function," PhD thesis, Technischen Universität Dresden, 2005.

[37] M. Avila, S. Begot, F. Duculty, and T. S. Nguyen, "2d image based road pavement crack detection by calculating minimal paths and dynamic programming," in *Image Processing (ICIP), 2014 IEEE International Conference on*, IEEE, 2014, pp. 783–787.

[38] R. Amhaz, S. Chambon, J. Idier, and V. Baltazart, "A new minimal path selection algorithm for automatic crack detection on pavement images," in *Image Processing (ICIP), 2014 IEEE International Conference on*, IEEE, 2014, pp. 788–792.

[39] R. Amhaz, S. Chambon, J. Idier, and V. Baltazart, "Automatic crack detection on two-dimensional pavement images: An algorithm based on minimal path selection," *IEEE Transactions on Intelligent Transportation Systems*, vol. 17, no. 10, pp. 2718–2729, 2016.

[40] H. Lee and J. Kim, "Development of a crack type index," *Transportation Research Record: Journal of the Transportation Research Board*, no. 1940, pp. 99–109, 2005.

[41] K. Kirschke and S. Velinsky, "Histogram-based approach for automated pavement-crack sensing," *Journal of Transportation Engineering*, vol. 118, no. 5, pp. 700–710, 1992.

[42] H. Koutsopoulos and A. Downey, "Primitive-based classification of pavement cracking images," *Journal of Transportation Engineering*, vol. 119, no. 3, pp. 402–418, 1993.

[43] J. Chou, W. A. O'Neill, and H. Cheng, "Pavement distress classification using neural networks," in *Systems, Man, and Cybernetics, 1994. Humans, Information and Technology., 1994 IEEE International Conference on*, IEEE, vol. 1, 1994, pp. 397–401.

[44] K. M. Chua and L. Xu, "Simple procedure for identifying pavement distresses from video images," *Journal of transportation engineering*, vol. 120, no. 3, pp. 412–431, 1994.

[45] H Lee and H Oshima, "New crack-imaging procedure using spatial autocorrelation function," *Journal of Transportation Engineering*, vol. 120, no. 2, pp. 206–228, 1994.

[46] A Georgopoulos, A Loizos, and A Flouda, "Digital image processing as a tool for pavement distress evaluation," *ISPRS Journal of Photogrammetry and Remote Sensing*, vol. 50, no. 1, pp. 23–33, 1995.

[47] J. Laurent, M. Talbot, and M. Doucet, "Road surface inspection using laser scanners adapted for the high precision 3d measurements of large flat surfaces," in *3-D Digital Imaging and Modeling, 1997. Proceedings., International Conference on Recent Advances in*, IEEE, 1997, pp. 303–310.

[48] H. Oh, N. W. Garrick, and L. E. Achenie, "Segmentation algorithm using iterative clipping for processing noisy pavement images," in *Imaging Technologies: Techniques and Applications in Civil Engineering. Second International ConferenceEngineering Foundation; and Imaging Technologies Committee of the Technical Council on Computer Practices, American Society of Civil Engineers.*, 1998.

[49] H.-D. Cheng and M. Miyojim, "Automatic pavement distress detection system," *Information Sciences*, vol. 108, no. 1-4, pp. 219–240, 1998.

[50] J. Iivarinen and A. Visa, "An adaptive texture and shape based defect classification," in *Pattern Recognition, 1998. Proceedings. Fourteenth International Conference on*, IEEE, vol. 1, 1998, pp. 117–122.

[51] H. Cheng, J.-R. Chen, C. Glazier, and Y. Hu, "Novel approach to pavement cracking detection based on fuzzy set theory," *Journal of Computing in Civil Engineering*, vol. 13, no. 4, pp. 270–280, 1999.

[52] H Cheng, X Jiang, J Li, and C Glazier, "Automated real-time pavement distress analysis," *Transportation Research Record: Journal of the Transportation Research Board*, no. 1655, pp. 55–64, 1999.

[53] D. Ryu, T. Choi, Y. Kim, and S. Nahm, "Measurement of the fatigue-crack using image processing techniques," in *Knowledge-Based Intelligent Engineering Systems and Allied Technologies, 2000. Proceedings. Fourth International Conference on*, IEEE, vol. 1, 2000, pp. 121–124.

[54] K. C. Wang and W. Gong, "Real-time automated survey of pavement surface distress," in *Applications of Advanced Technologies in Transportation (2002)*, 2002, pp. 465–472.

[55] H. Cheng, X. Shi, and C Glazier, "Real-time image thresholding based on sample space reduction and interpolation approach," *Journal of computing in civil engineering*, vol. 17, no. 4, pp. 264–272, 2003.

[56] B. Xu and Y. Huang, "Automated pavement cracking rating system: A summary," *Center for Transportation Research The University of Texas at Austin*, 2003.

[57] D. H. Ryu and S. H. Nahm, "Image processing techniques applied to automatic measurement of the fatigue-crack," in *Key Engineering Materials*, Trans Tech Publ, vol. 297, 2005, pp. 34–39.

[58] J. Bray, B. Verma, X. Li, and W. He, "A neural network based technique for automatic classification of road cracks," in *Neural Networks, 2006. IJCNN'06. International Joint Conference on*, IEEE, 2006, pp. 907–912.

[59] N. Sy, M. Avila, S. Begot, and J.-C. Bardet, "Detection of defects in road surface by a vision system," in *Electrotechnical Conference, 2008. MELECON 2008. The 14th IEEE Mediterranean*, IEEE, 2008, pp. 847–851.

[60] J Laurent, D Lefebvre, and E Samson, "Development of a new 3d transverse laser profiling system for the automatic measurement of road cracks," in *Symposium on Pavement Surface Characteristics, 6th, 2008, Portoroz, Slovenia*, 2008.

[61] H. Oliveira and P. L. Correia, "Identifying and retrieving distress images from road pavement surveys," in *Image Processing, 2008. ICIP 2008. 15th IEEE International Conference on*, IEEE, 2008, pp. 57–60.

[62] K. Rajan, "Analysis of pavement condition data employing principal component analysis and sensor fusion techniques," PhD thesis, Kansas State University, 2008.

[63] T Saar and O Talvik, "Automatic asphalt pavement crack detection and classification using neural networks," in *Electronics Conference (BEC), 2010 12th Biennial Baltic*, IEEE, 2010, pp. 345–348.

[64] E Salari and G Bao, "Pavement distress detection and severity analysis," in *Proc. SPIE*, vol. 7877, 2011, p. 78770C.

[65] M. R. Jahanshahi, F. Jazizadeh, S. F. Masri, and B. Becerik-Gerber, "Unsupervised approach for autonomous pavement-defect detection and quantification using an inexpensive depth sensor," *Journal of Computing in Civil Engineering*, vol. 27, no. 6, pp. 743–754, 2012.

[66] H. Oliveira and P. L. Correia, "Automatic road crack detection and characterization," *IEEE Transactions on Intelligent Transportation Systems*, vol. 14, no. 1, pp. 155–168, 2013.

[67] F.-C. Chen, M. R. Jahanshahi, R.-T. Wu, and C. Joffe, "A texture-based video processing methodology using bayesian data fusion for autonomous crack detection on metallic surfaces," *Computer-Aided Civil and Infrastructure Engineering*, vol. 32, no. 4, pp. 271–287, 2017.

[68] R. Salini, B. Xu, and M. Souliman, "Impact of image resolution on pavement distress detection using picucha methodology," *Stavební Obzor-The Civil Engineering Journal*, vol. 25, no. 4, 2016.

[69] G. Lu, Q. Zhao, J. Liao, and Y. He, "Pavement crack identification based on automatic threshold iterative method," in *Seventh International Conference on Electronics and Information Engineering*, International Society for Optics and Photonics, 2017, 103221F–103221F.

[70] R. Salini, B. Xu, and P. Paplauskas, "Pavement distress detection with picucha methodology for area-scan cameras and dark images," *Stavební Obzor-The Civil Engineering Journal (1)*, pp. 34–45, 2017.

[71] M. Eisenbach, R. Stricker, D. Seichter, K. Amende, K. Debes, M. Sesselmann, D. Ebersbach, U. Stoeckert, and H.-M. Gross, "How to get pavement distress detection ready for deep learning? a systematic approach," in *Neural Networks (IJCNN), 2017 International Joint Conference on*, IEEE, 2017, pp. 2039–2047.

[72] S. Chaudhury, G. Nakano, J. Takada, and A. Iketani, "Spatial-temporal motion field analysis for pixelwise crack detection on concrete surfaces," in *Applications of Computer Vision (WACV), 2017 IEEE Winter Conference on*, IEEE, 2017, pp. 336–344.

[73] J. Song, H. Gao, Y. Liu, and Y Yu, "Road damage identification and degree assessment based on ugv," *International Journal on Smart Sensing and Intelligent Systems*, vol. 9, no. 4, pp. 2069–2087, 2016.

[74] A. Tedeschi and F. Benedetto, "A real-time automatic pavement crack and pothole recognition system for mobile android-based devices," *Advanced Engineering Informatics*, vol. 32, pp. 11–25, 2017.

[75] Y. Maode, B. Shaobo, X. Kun, and H. Yuyao, "Pavement crack detection and analysis for high-grade highway," in *Electronic Measurement and Instruments, 2007. ICEMI'07. 8th International Conference on*, IEEE, 2007, pp. 4–548.

[76] A. Ayenu-Prah and N. Attoh-Okine, "Evaluating pavement cracks with bidimensional empirical mode decomposition," *EURASIP Journal on Advances in Signal Processing*, vol. 2008, no. 1, p. 861 701, 2008.

[77] B.-C. Sun and Y.-j. Qiu, "Automatic identification of pavement cracks using mathematic morphology," in *International Conference on Transportation Engineering 2007*, 2007, pp. 1783–1788.

[78] L. Ying and E. Salari, "Beamlet transform based technique for pavement image processing and classification," in *Electro/Information Technology, 2009. eit'09. IEEE International Conference on*, IEEE, 2009, pp. 141–145.

[79] L Ying and E Salari, "Beamlet transform-based technique for pavement crack detection and classification," *Computer-Aided Civil and Infrastructure Engineering*, vol. 25, no. 8, pp. 572–580, 2010.

[80] F. M. Nejad and H. Zakeri, "An optimum feature extraction method based on wavelet–radon transform and dynamic neural network for pavement distress classification," *Expert Systems with Applications*, vol. 38, no. 8, pp. 9442–9460, 2011.

[81] F. M. Nejad and H Zakeri, "An expert system based on wavelet transform and radon neural network for pavement distress classification," *Expert Systems with Applications*, vol. 38, no. 6, pp. 7088–7101, 2011.

[82] C. A. Lettsome, Y.-C. Tsai, and V. Kaul, "Enhanced adaptive filter-bank-based automated pavement crack detection and segmentation system," *Journal of Electronic Imaging*, vol. 21, no. 4, pp. 043 008–043 008, 2012.

[83] A. Ouyang and Y. Wang, "Edge detection in pavement crack image with beamlet transform," in *2nd International Conference on Electronic & Mechanical Engineering and Information Technology*, Atlantis Press, 2012.

[84] B Santhi, G Krishnamurthy, S Siddharth, and P. Ramakrishnan, "Automatic detection of cracks in pavements using edge detection operator," *Journal of Theoretical and Applied Information Technology*, vol. 36, no. 2, pp. 199–205, 2012.

[85] Y.-S. Su, S.-C. Kang, J.-R. Chang, and S.-H. Hsieh, "Dual-light inspection method for automatic pavement surveys," *Journal of Computing in Civil Engineering*, vol. 27, no. 5, pp. 534–543, 2012.

[86] E. Zalama, J. Gómez-García-Bermejo, R. Medina, and J. Llamas, "Road crack detection using visual features extracted by gabor filters," *Computer-Aided Civil and Infrastructure Engineering*, vol. 29, no. 5, pp. 342–358, 2014.

[87] L. Zeng, X. Shi, Y. Li, and J. Wang, "Pavement crack recognition based wireless video sensors," in *CICTP 2015*, 2015, pp. 2286–2294.

[88] W. Li, J. Huyan, S. L. Tighe, Q.-q. Ren, and Z.-y. Sun, "Three-dimensional pavement crack detection algorithm based on two-dimensional empirical mode decomposition," *Journal of Transportation Engineering, Part B: Pavements*, vol. 143, no. 2, p. 04 017 005, 2017.

[89] G. Shen, "Road crack detection based on video image processing," in *Systems and Informatics (ICSAI), 2016 3rd International Conference on*, IEEE, 2016, pp. 912–917.

[90] A. Kumar and G. K. Pang, "Defect detection in textured materials using gabor filters," *IEEE Transactions on industry applications*, vol. 38, no. 2, pp. 425–440, 2002.

[91] J. Zhou, P. S. Huang, and F.-P. Chiang, "Wavelet-aided pavement distress image processing," in *Wavelets: Applications in signal and image processing X*, International Society for Optics and Photonics, vol. 5207, 2003, pp. 728–740.

[92] J.-H. Lee, H.-S. Yoo, Y.-S. Kim, J.-B. Lee, and M.-Y. Cho, "The development of a machine vision-assisted, teleoperated pavement crack sealer," *Automation in construction*, vol. 15, no. 5, pp. 616–626, 2006.

[93] Y. Sun, E. Salari, and E. Chou, "Automated pavement distress detection using advanced image processing techniques," in *Electro/Information Technology, 2009. Eit'09. IEEE International Conference on*, IEEE, 2009, pp. 373–377.

[94] Q. Li, M. Yao, X. Yao, and B. Xu, "A real-time 3d scanning system for pavement distortion inspection," *Measurement Science and Technology*, vol. 21, no. 1, p. 015 702, 2009.

[95] X. Yao, M. Yao, and B. Xu, "Automated measurements of road cracks using line-scan imaging," *Journal of Testing and Evaluation*, vol. 39, no. 4, pp. 621–629, 2011.

[96] B. Qian, Z. Tang, and W. Xu, "Pavement crack detection based on improved tensor voting," in *Computer Science & Education (ICCSE), 2014 9th International Conference on*, IEEE, 2014, pp. 397–402.

[97] C. Jiang and Y. J. Tsai, "Enhanced crack segmentation algorithm using 3d pavement data," *Journal of Computing in Civil Engineering*, vol. 30, no. 3, p. 04 015 050, 2015.

[98] B. Peng, Y. Fu, and Y.-s. Jiang, "De-noising algorithm for pavement crack images based on bi-layer connectivity checking," *Journal of Highway and Transportation Research and Development (English Edition)*, pp. 18–25, 2016.

[99] T. Yu, A. Zhu, and Y. Chen, "Efficient crack detection method for tunnel lining surface cracks based on infrared images," *Journal of Computing in Civil Engineering*, vol. 31, no. 3, p. 04 016 067, 2016.

[100] S. Mokhtari, L. Wu, and H.-B. Yun, "Statistical selection and interpretation of imagery features for computer vision-based pavement crack–detection systems," *Journal of Performance of Constructed Facilities*, vol. 31, no. 5, p. 04 017 054, 2017.

[101] V. Kaul, A. Yezzi, and Y. Tsai, "Detecting curves with unknown endpoints and arbitrary topology using minimal paths," *IEEE Transactions on Pattern Analysis and Machine Intelligence*, vol. 34, no. 10, pp. 1952–1965, 2012.

[102] Q. Li, Q. Zou, D. Zhang, and Q. Mao, "Fosa: F* seed-growing approach for crack-line detection from pavement images," *Image and Vision Computing*, vol. 29, no. 12, pp. 861–872, 2011.

[103] Y. J. Tsai, C. Jiang, and Z. Wang, "Pavement crack detection using high-resolution 3d line laser imaging technology," in *7th RILEM International Conference on Cracking in Pavements*, Springer, 2012, pp. 169–178.

[104] Y. J. Tsai, V. Kaul, and A. Yezzi, "Automating the crack map detection process for machine operated crack sealer," *Automation in Construction*, vol. 31, pp. 10–18, 2013.

[105] H. Nguyen, T. Kam, and P. Cheng, "Automatic crack detection from 2d images using a crack measure-based b-spline level set model," *Multidimensional Systems and Signal Processing*, pp. 1–32, 2016.

[106] H. Nguyen, L. Nguyen, and D. N. Sidorov, "A robust approach for road pavement defects detection and classification," *Journal of Computational and Engineering Mathematics*, vol. 3, no. 3, pp. 40–52, 2016.

[107] M. Hao, C. Lu, G. Wang, and W. Wang, "An improved neuron segmentation model for crack detection–image segmentation model," *Cybernetics and Information Technologies*, vol. 17, no. 2, pp. 119–133, 2017.

[108] S. Li, Y. Cao, and H. Cai, "Automatic pavement-crack detection and segmentation based on steerable matched filtering and an active contour model," *Journal of Computing in Civil Engineering*, vol. 31, no. 5, p. 04 017 045, 2017.

[109] X. Feng, R. Mathurin, and S. A. Velinsky, "Practical, interactive, and object-oriented machine vision for highway crack sealing," *Journal of transportation engineering*, vol. 131, no. 6, pp. 451–459, 2005.

[110] A. Zhang, Q. Li, K. Wang, and S. Qiu, "Matched filtering algorithm for pavement cracking detection," *Transportation Research Record: Journal of the Transportation Research Board*, no. 2367, pp. 30–42, 2013.

[111] Y.-C. Tsai and A. Chatterjee, "Comprehensive, quantitative crack detection algorithm performance evaluation system," *Journal of Computing in Civil Engineering*, vol. 31, no. 5, p. 04 017 047, 2017.